ABSTRACT

Title of dissertation: ADAPTIVE FLIGHT AND ECHOLOCATION BEHAVIOR IN BATS

Benjamin Mather Falk, Doctor of Philosophy, 2015

Dissertation directed by: Professor Cynthia F. Moss
Program in Neuroscience and Cognitive Science

Bats use sonar to identify and localize objects as they fly and navigate in the dark. They actively adjust the timing, intensity, and frequency content of their sonar signals in response to task demands. They also control the directional characteristics of their sonar vocalizations with respect to objects in the environment. Bats demonstrate highly maneuverable and agile flight, producing high turn rates and abrupt changes in speed, as they travel through the air to capture insects and avoid obstacles. Bats face the challenge of coordinating flight kinematics with sonar behavior, as they adapt to meet the varied demands of their environment.

This thesis includes three studies, one on the comparison of flight and echolocation behavior between an open space and a complex environment, one on the coordination of flight and echolocation behavior during climbing and turning, and one on the flight kinematic changes that occur under wind gust conditions.

In the first study, we found that bats adapt the structure of the sonar signals, temporal patterning, and flight speed in response to a change in their environment. We also found that flight stereotypy developed over time in the more complex environment, but not to the extent expected from previous studies of non-foraging bats. We found that the sonar beam aim of the bats predicted flight turn rate, and that the relationship changed as the bats reacted to the obstacles. In the second study, we characterized the coordination of flight and sonar behavior as bats made a steep climb and sharp turns while they navigated a net obstacle. We found the coordinated production of sonar pulses with the wingbeat phase became altered during navigation of tight turns. In the third study, we found that bats adapt wing kinematics to perform under wind gust conditions.

By characterizing flight and sonar behaviors in an insectivorous bat species, we find evidence for tight coordination of sensory and motor systems for obstacle navigation and insect capture. Through these studies, we learn about the mechanisms by which mammals and other organisms process sensory information to adapt their behaviors.

ADAPTIVE FLIGHT AND ECHOLOCATION BEHAVIOR IN BATS

By

Benjamin Mather Falk

Dissertation submitted to the Faculty of the Graduate School of the
University of Maryland, College Park, in partial fulfillment
of the requirements for the degree of
Doctor of Philosophy
2015

Advisory Committee:
Professor Cynthia F. Moss, Chair
Professor Catherine Carr
Professor Jens Herberholz
Professor Timothy Horiuchi
Professor David Yager

Acknowledgments

I thank Cindy Moss for discussing papers, editing many versions of manuscripts, encouraging my interests, and training me to become a scientist. I thank Tameeka Williams for welcoming me to join her texture discrimination project, my first collaboration, which started me along this path. I thank Murat Aytekin for his approach to asking questions and his assistance whenever I asked. I thank Kaushik Ghose for his software tools, his microphone array, his help building batkeeping, and his positive attitude. I thank all the Batlab members, for their help and their friendship. I thank my collaborators including Lasse Jakobsen, Annemarie Surlykke, Yossi Yovel, and Nachum Ulanovsky. I thank my committee for their feedback and support. I thank my parents, Craig Falk and Sarah Mather, who supported and encouraged my endeavors. And I thank my wife, Jessica Nelson, for her patience and care.

Table of Contents

List of Tables

List of Figures

Chapter 1: Introduction

Bats are highly diverse, with over 1200 species, comprising more than a fifth of mammals (N. B. Simmons, 2005). Bats occur across varied habitats, from the tropics to the desert, and fill many ecological niches, as they forage on fruit, nectar, fish, insects, blood, or meat. Each species is adapted to its environment, from the sonar calls they use to the flight behaviors they perform. Some species are specialized for fast, long-distance flight, while others for slow, maneuvering, or even hovering flight. Flight and sonar behaviors are adapted together to suit different foraging styles, whether it is gleaning or open-space foraging, across cluttered or open environments (Schnitzler & Kalko, 2001).

Echolocation

Active sensing is the process in which animals purposefully guide their sensory systems to seek out information from the environment. In vision research, the study of active sensing examines the role of eye and/or head movements on perception (Aloimonos, Weiss, & Bandyopadhyay, 1988; Yarbus, Haigh, & Rigss, 1967). Electrolocating fish generate electric fields and sense changes in the field to perceive their surroundings (von der Emde, 1999). Many animals navigate in the dark by active touching, including insects with antennae (Staudacher, Gebhardt, & Dürr, 2005) and rodents with whiskers (Catania & Henry, 2006; Diamond, von Heimendahl, Knutsen, Kleinfeld, & Ahissar, 2008; Mitchinson et al., 2011). Biological sonar, or echolocation, is a form of active sensing in which an animal generates sounds, which propagate through the environment and return as reflections from objects. Echolocating animals include toothed whales,

which produce ultrasonic sounds underwater (Au, 1993), bats, which produce ultrasonic sounds in air to navigate at night (Griffin, 1958), at least two groups of birds, the Oilbird and the swiftlets (Brinkløv, Fenton, & Ratcliffe, 2013), which produce sounds audible to humans, and to a limited extent, humans (Rice, 1967; Stroffregen & Pittenger, 1995).

Most echolocating bats produce sonar pulses by passing air over their vibrating vocal cords, similar to human sound production. However, one suborder of bats, *Pteropodidae*, is not capable of laryngeal echolocation, and instead, relies mostly on other senses for navigation in the dark. Within this suborder, one genus, *Rousettus*, has secondarily evolved echolocation and produce ultrasound tongue clicks to navigate (Holland, Waters, & Rayner, 2004; Neuweiler, 2000). The large diversity of animals using echolocation assures a wide and varied behavioral repertoire.

Laryngeal echolocating bats produce one of two types of sonar signals, frequency-modulated (FM) or constant-frequency (CF) signals, emitted either through the nose or mouth. CF emitting bat species produce pure tones, typically of long duration, and utilize Doppler shifts in the returning echoes to locate prey created by movement (e.g. the fluttering wings of a moth) (Bell & Fenton, 1984; Schnitzler, 1968; von der Emde & Schnitzler, 1990). Bats emitting FM signals produce sounds which vary in intensity and frequency over time. FM signals return echoes, which can be cross correlated with a copy of the emitted sound, for precise object localization (J. A. Simmons, 1973). All bats which produce CF signals often add short FM components to their sonar signals to aid in target localization.

As an FM echolocating bat generates sounds in its environment, it adjusts the duration, intensity, frequency, and directionality of its sonar calls. Bats reduce call duration to avoid pulse-echo overlap with nearby objects (Cahlander, McCue, & Webster, 1964; Kalko & Schnitzler, 1989; Schnitzler, Kalko, Miller, & Surlykke, 1987), widen call bandwidth to better localize objects (Faure & Barclay, 1994; Hartley, 1992; Kalko & Schnitzler, 1993; Surlykke et al., 1993), reduce call intensity as they approach objects as a method for keeping target echo strength constant (Hartley, 1992; Hiryu, Hagino, Riquimaroux, & Watanabe, 2007), and decrease directionality to widen the field of view as they attack prey (Jakobsen & Surlykke, 2010).

Bats also adjust the timing pattern of their sonar sounds as they approach a target or as they operate in different environments. When searching for food in open space, bats emit sounds at a slow rate of 5-10 Hz (Griffin, 1958; Surlykke & Moss, 2000). When they near an insect or fly amidst clutter, they increase the rate of sound production, augmenting the rate of echo information updates per unit time (Moss & Surlykke, 2001). As bats capture an insect or prepare to land, they emit a terminal buzz, in which sounds are produced at a rate as high as 200 Hz, which is about 20 times the rate of the big brown bat's wingbeat cycle.

Bats also control the returning echo information about their environment by adjusting the aim of their sonar sounds and adapting the width of their sonar beam. Bat sonar sounds are directional (Hartley & Suthers, 1989; Jakobsen, Ratcliffe, & Surlykke, 2013; J. A.

Simmons, 1969), which restricts the animal's view of 3D space. Bats must therefore control the aim of the sonar beam to spatially sample the environment and objects of interest (Falk, Williams, Aytekin, & Moss, 2011; Ghose & Moss, 2003; Seibert, Koblitz, Denzinger, & Schnitzler, 2013; Surlykke, Ghose, & Moss, 2009). Recent evidence demonstrates that bats control the width of their sonar beam, by lowering their emitted sound frequency, to increase the field of view during insect capture (Jakobsen & Surlykke, 2010).

As bats adapt multiple parameters of their sonar signals to extract information about their environment, the specific vocal behaviors observed can be used to infer internal processes such as target selection and attention. As bats adjust the timing, frequency, intensity, and directionality to perform in different behavioral tasks, we can attribute these changes in behavior to attentional control and motivated actions (Ghose & Moss, 2006).

Flight

Three extant groups of animals, insects, birds, and bats, have evolved powered flight. A diversity of behaviors has evolved within these groups for variety of purposes, e.g. hunting, evading capture, and maneuvering around objects.

Flight requires balancing four basic physical forces, lift, drag, thrust, and weight. Lift must be generated in order to maintain altitude and overcome the weight of the animal. When moving through a medium, an animal will also experience drag, a force acting in

the opposite direction of the movement, which is due to the viscosity of the fluid, in this case, the air. Wings can only generate lift when air moves around them, so an animal needs to overcome the force of drag. This forward force is called thrust, which propels the animal through the medium. In animal flight, thrust is generated through the flapping wings. Air that moves faster has less pressure than air that moves slower. As the wing is propelled forward, and by altering wing shape or angle of attack (angle the wing is pointed in relation to air flow), air will move faster or slower across the top of the wing relative to the bottom of the wing, generating a larger or smaller lift force. The following equations specify the aerodynamic forces lift, L, and drag, D, according to fixed wing theory, as:

$$L = C_L \frac{\rho U^2}{2} A \tag{1.1}$$

and

$$D = C_D \frac{\rho U^2}{2} A \tag{1.2}$$

where C_L is the lift coefficient and C_D is the drag coefficient, ρ is the density in air, U is the flight speed, and A is the wing area. This lift force is proportional to the square of the difference in air speed between the top and the bottom of the wing, so small changes to the camber or angle of attack can result in large changes in lift.

Increasing angle of attack will generate greater lift. However, increasing too much will eventually result in stall, as the airflow over the upper surface detaches from the wing, creating a turbulent wake, which increases drag and reduces lift. The critical angle for stall differs among animals: large birds (20 degrees), grasshoppers (30 degrees), fruit flies

(50 degrees) (Alexander, 2002). The critical angle depends partly on airfoil shape and partly on the Reynolds number, which is the ratio of inertial forces to viscous forces. A well-timed stall can be beneficial in some circumstances, like landing.

Vortices are created during flight. A bound vortex is created by the wing moving through the air as air passes below and above the wing. The air stays close to the wing, especially at low angles of attack. A starting vortex rolls off the trailing edge and turns in the opposite direction to the bound vortex when the wing first develops lift (Alexander, 2002). Trailing vortices (also called tip vortices) are created and stream off the end of each wing and trail behind the wing as the wing produces lift. Trailing vortices cause an additional type of drag, called induced drag. The viscosity of the medium eventually causes the tip and starting vortices to die out. Flapping flight can generate a more complex vortex wake than just tip and starting vortices, such as leading edge vortices. These vortices can be studied using a method called particle image velocimetry (PIV). Using PIV, researchers illuminate and image small particles in the air behind the animal to recreate the wake profile (Hedenström et al., 2007; Hubel, Hristov, Swartz, & Breuer, 2009). By studying the wake profile, one can deduce the aerodynamic forces used.

The fixed wing theory of flight does not fully explain the lift forces generated by flapping animals (Hedenström et al., 2007; Hedenström & Johansson, 2015). Lift changes with the camber, angle of attack, wing area, and stiffness of the wing, which changes within the wing beat for flapping animals. A number of theories have been proposed to better explain flapping flight. In the blade-element theory, first proposed by Weis-Fogh &

Jensen (1956), the total aerodynamic force is determined by integrating instantaneous forces along the wingbeat as in equations 1.1 and 1.2. With relatively simple wingbeat kinematics and wing geometries, this is a suitable strategy, but for bats, which have complex kinematics and wing shape distortion, this model is not sufficient. Norberg (1976) discovered that the quasi-steady state model fails to explain the entirety of lift required for slow, maneuvering flight, thus, unsteady effects must be present. Recent studies of vertebrate flight have focused on one particular unsteady mechanism for generating lift, the leading edge vortex (LEV) (Muijres et al., 2008; Muijres, Johansson, Winter, & Hedenström, 2014) The LEV is created on the leading edge of the wing, during slow flight, and can contribute a large percentage of lift despite high angles of attack and slow air speed. Insects (Ellington, van den Berg, Willmott, & Thomas, 1996) and birds (Warrick, Tobalske, & Powers, 2005) also use the LEV. The LEV has not yet been found to occur in bats during cruising flight speed. This is likely due to the fact that the LEV generates significant drag, and would be of greatest benefit during slow flight. Of the more than 1200 species of bats, only four have had detailed wake profiles rigorously studied: *Cynopterus brachyotis* (Hubel et al., 2009; Hubel, Riskin, Swartz, & Breuer, 2010), *Tadarida brasiliensis* (Hubel, Hristov, Swartz, & Breuer, 2012), and the closely related bats *Glossophaga soricina* and *Leptonycteris curasoa* (Hubel et al., 2009; Muijres, Johansson, Winter, & Hedenström, 2011). The species, *T. brasiliensis*, is a high-altitude, fast-flying, insectivore, with a high wing aspect ratio, and likely does not represent more common bat fliers.

Sensorimotor integration of echolocation and flight

The sensory and motor systems that bats use are linked – the bat processes echo information to generate appropriate flight motor output in order to complete different tasks, and the flight motor behavior also sets spatial boundaries on future sensory input. The bat constructs a flight plan based on information it has gathered from its echo sensing perception, and flight motor output is guided by sensory input through a delayed linear control law (Ghose & Moss, 2006). However, bats sometimes rely on spatial memory for path planning, and reduce sonar pulse production in this circumstance (Barchi, Knowles, & Simmons, 2013). There are many reports of bats colliding with obstacles which should have been detected by echolocation and avoided (Crawford & Baker, 1981; Gelder, 1956; Nicholson, Tankersley Jr, Fiedler, & Nicholas, 2005), suggesting that bats may not attend to the echo information returning to them. Thus, the bat's sensory system can be guided by flight, as well as suppressed by memory and attention. In motor control aspect of biosonar, the production, timing, and intensity of the sonar pulses is modulated by the flight behavior related to wing beat (Koblitz, Stilz, & Schnitzler, 2010). Other sensory feedback (touch, smell, vision) can also contribute to the bat's perception of space. Bats integrate sensory information together with motor output into a cohesive system for navigating their environment.

The big brown bat

The experiments in this dissertation were conducted with the big brown bat, *Eptesicus fuscus* (Palisot de Beauvois 1796). The big brown bat uses FM signals which sweep in frequency between 20-110 kHz (Griffin, 1958; Neuweiler, 2000). *E. fuscus* is an aerial

hawking open-space forager, but also forages for insects in cluttered environments (J. A. Simmons, Eastman, Horowitz, O'Farrell, & Lee, 2001). Its adaptable echolocation system is capable of detecting prey at long range in open spaces (Surlykke & Moss, 2000) and also capable of navigating through obstacles and clutter at short range (Moss, Bohn, Gilkenson, & Surlykke, 2006), making this species well suited for studies of flight and echolocation. *E. fuscus* has an aspect ratio between 6.4-7 (Farney & Fleharty, 1969; Norberg & Rayner, 1987), above the average for the family Vespertilionidae (Bininda-Emonds & Russell, 1994; Norberg & Rayner, 1987). The big brown bat has been widely studied across varied flight and echolocation experiments, including clutter navigation (Moss et al., 2006), wire avoidance (Sändig, Schnitzler, & Denzinger, 2014), and obstacle chain arrays (Barchi et al., 2013; Petrites, Eng, Mowlds, Simmons, & DeLong, 2009), as well as in the field under natural conditions (Surlykke & Moss, 2000).

Overview of experiments

The results of this dissertation demonstrate that the big brown bat is capable of jointly adapting echolocation and flight behavior to meet different task requirements. Three experiments were conducted in a large flight room, each with separate demands on flight and echolocation.

The first experiment, presented in chapter 2, explores how bats meet the demands of a challenging navigation task during foraging. Adjustments to the bat's flight motor output and sonar sampling behavior were examined as the bat transitioned from an open space to a cluttered environment. Changes in the temporal patterning and sonar call structure

were found to coincide with the environment in which the bats were tested. Bats flew slower in the cluttered environment, and a linking relationship between the direction angle of sonar calls and flight motor output also changed in the cluttered space. Bats were tested over multiple days, and flight stereotypy was found, but no change in sonar call behavior was observed over time.

The second experiment, presented in chapter 3, characterizes the echolocation and flight behavior during climbing and turning maneuvering. The bats were tasked with flying through a low entrance into a narrow corridor, making a sharp turn inside the corridor, then climbing upwards to the exit of the corridor, to finally make a sharp turn to capture the tethered insect. The bats adjusted both sonar and flight behavior as they maneuvered through this task.

The third experiment, presented in chapter 4, explores flight behavior of bats as they overcome gusts of wind to navigate an obstacle. Bats had high performance in the task even with wind gusts. Detailed flight kinematics and trajectory analysis reveal changes in the flight behavior with the wing gusts. The results of this study reveal that bats make rapid adaptive changes in flight kinematics to successfully maneuver under wind gust conditions.

Chapter 2 has been published as:

Bats coordinate sonar and flight behavior as they forage in open and cluttered environments

Falk, B., Jakobsen, L., Surlykke, A., & Moss, C. F.
(2014). The Journal of Experimental Biology, 4356–4364.

Chapter 2: Bats coordinate sonar and flight behavior as they forage in open and cluttered environments

Abstract

Echolocating bats use active sensing as they emit sounds and listen to the returning echoes to probe their environment for navigation, obstacle avoidance, and pursuit of prey. The sensing behavior of bats includes the planning of 3D spatial trajectory paths, which are guided by echo information. In this study, we examined the relationship between active sonar sampling and flight motor output as bats changed environments from open space to an artificial forest in a laboratory flight room. Using high-speed video and audio recordings, we reconstructed and analyzed 3D flight trajectories, sonar beam aim and acoustic sonar emission patterns as the bats captured prey. We found that big brown bats adjusted their sonar call structure, temporal patterning, and flight speed in response to environmental change. The sonar beam aim of the bats predicted the flight turn rate in both the open room and the forest. However, the relationship between sonar beam aim and turn rate changed in the forest during the final stage of prey pursuit, during which the bat made shallower turns. We found flight stereotypy developed over multiple days in the forest, but did not find evidence for a reduction in active sonar sampling with experience. The temporal patterning of sonar sound groups was related to path planning around obstacles in the forest. Together, these results contribute to our understanding of how bats coordinate echolocation and flight behavior to represent and navigate their environment.

Introduction

Echolocating bats actively probe the environment with ultrasonic signals to build a spatial representation of a sonar scene from information carried by returning echoes (Griffin, 1958). Each scene is dynamic: the animal and its prey are moving through space, which produces changes in the features of echo returns. The task is further complicated in a cluttered environment where each sonar emission results in a cascade of echoes arriving from different locations, which the bat must organize into a coherent representation (Moss et al., 2006; Moss, Chiu, & Surlykke, 2011; J. A. Simmons, Kick, Moffat, Masters, & Kon, 1988). Acoustic cues, such as interaural time, intensity, and spectral differences, provide information about the direction of a sonar object (Shimozawa, Suga, Hendler, & Schuetze, 1974; J. A. Simmons et al., 1983), whereas echo arrival time provides information about its distance (Hartridge, 1945; J. A. Simmons, 1973). The bat's own actions, coupled with information carried by dynamic echo streams, may be key to understanding how the bat can operate in a complex environment.

There are over 1200 species of bats (N. B. Simmons, 2005), of which approximately 70% echolocate using the larynx (Jones & Teeling, 2006). These species have evolved varied biosonar signal designs to enable successful foraging in their natural habitats (Schnitzler & Kalko, 2001). Detecting prey, parsing the acoustic scene, and localizing objects require sonar signals tailored to each task. Bats that emit short-frequency-modulated calls of low duty cycle to capture insects on the wing reduce the duration of calls in cluttered environments to minimize pulse-echo overlap (Cahlander et al., 1964; Kalko & Schnitzler, 1989; Schnitzler et al., 1987), and widen call bandwidth to increase

information about object location (Faure & Barclay, 1994; Hartley, 1992; Jensen & Miller, 1999; Kalko & Schnitzler, 1993; Surlykke et al., 1993). These bats also adjust the interval between successive calls to receive echoes from relevant objects before producing the next call (Moss & Surlykke, 2001; Surlykke & Moss, 2000). This serves to avoid ambiguity about the echo arrival time from each sonar emission. In highly cluttered environments where pulse intervals (PIs) cannot be adequately adapted to avoid ambiguity in call-echo assignment, bats make further adjustment in spectral structure of closely spaced calls in a group (Hiryu, Bates, Simmons, & Riquimaroux, 2010).

Although bats often decrease the interval of sounds in a continuous manner as they near obstacles, the temporal structure of sonar call sequences can be more complex. Occasionally, sound groups, clusters of several signals that contain a shorter PI than surrounding calls, occur embedded within a sequence of calls (Moss et al., 2006; Moss & Surlykke, 2001). Sound groups have been implicated in resolving spatial information in more detail (Kothari, Wohlgemuth, Hulgard, Surlykke, & Moss, 2014), and have been found to be more prevalent in complex acoustic scenes (Moss et al., 2006; Petrites et al., 2009; Sändig et al., 2014). These findings suggest that bats are actively controlling the features and timing of the sonar sounds they produce in order to build a representation of a complex environment; however, the echo scene, and thus the perception of the environment, is also dependent on the bat's own movement through space and time.

A more complete understanding of the echolocating bat's dynamic sonar scene must take into account the animal's active control of sonar signals in relation to its flight. Bat sonar

sounds are directional (Hartley & Suthers, 1989; Jakobsen et al., 2013; J. A. Simmons, 1969), which restricts the animal's view of 3D space. Bats must therefore control the aim of the sonar beam to spatially sample the environment and objects of interest (Falk et al., 2011; Ghose & Moss, 2003; Seibert et al., 2013; Surlykke et al., 2009). The sonar beam aim has been shown to predict flight motor output (Ghose & Moss, 2006). The time delay, or lag, between the sonar gaze angle and turn rate was found to be greater than zero for all phases of echolocation (Ghose & Moss, 2006). The gain, or slope, in the linear model predicting turn rate from gaze angle increased as the bats transitioned through the echolocation phases of insect capture. This adaptive linear relationship between acoustic gaze and flight behavior connects the bat's attentional control and motor planning behaviors. Together, these results indicate that the bat is guided by its spatial sampling of its environment, which is an interaction between the actively controlled sonar beam aim, the temporal patterning of its sonar signals, and its flight trajectory.

Here, we analyze the coordinated adjustments in echolocation and flight behavior of the insectivorous big brown bat, *Eptesicus fuscus* Palisot de Beauvois 1796 (Vespertilionidae), which forages in both open spaces as well as in and among vegetation (J. A. Simmons et al., 2001). We hypothesize that changes to the environment will result in adjustments to sonar signal design, sonar temporal patterning, sonar directional aim and flight steering and flight speed. Characterization of these adjustments can reveal adaptive behaviors for navigating clutter, the dynamics of echo information flow, and the representation of a bat's sonar scene.

Materials and Methods

Experimental setup and data collection

All experimental procedures were approved by the Institutional Animal Care and Use Committee at the University of Maryland, College Park. Experiments were conducted in a large flight room (flight area 6.0 m x 5.7 m x 2.5 m) lined with acoustic sound-absorbing foam (Sonex One, Acoustical Solutions, Inc.) in low, long wavelength light (>650 nm, incandescent light through infrared filters, Plexiglas G #2711, Atofina Chemicals). Animals used were nine adult, wild-caught *Eptesicus fuscus*, trained to catch insects (*Tenebrio molitor* larvae) tethered and hanging from the ceiling by monofilament fishing line (Berkley Trilene, 0.9 kg test, 0.13 mm diameter).

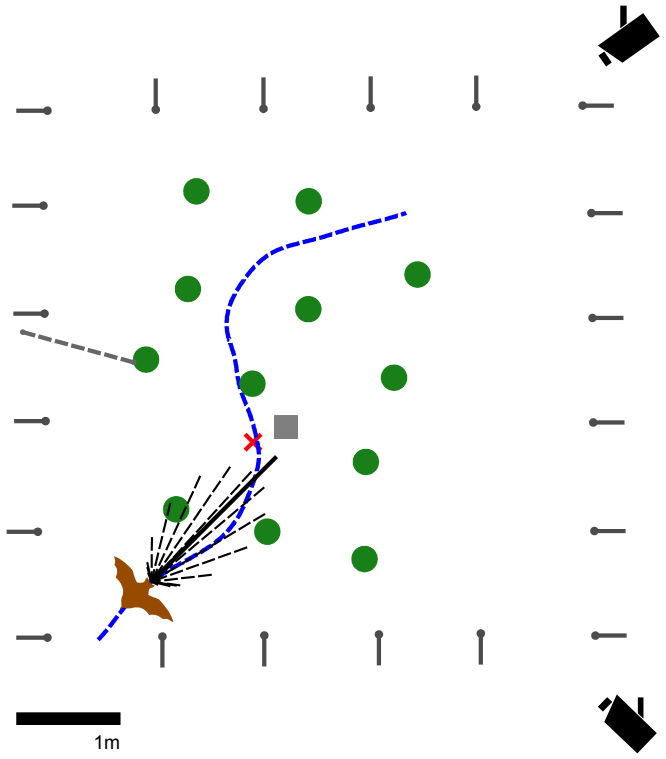

Fig. 2.1: Top view schematic of 'forest' flight room with artificial trees. The bat is represented in diagram, and the bat's flight path through the artificial trees shown as a dashed blue line. The tethered insect is represented as a red cross. The artificial trees are shown as green circles and, with respect to the room, plotted to scale. The left wall net is shown as a gray dashed line. The microphones from the planar array bordering the room are represented as gray circles. They are offset from the walls by 0.3 meter sticks, represented in gray. An example vocalization is depicted as the corrected intensity recorded at each of the microphones in the array (dashed black lines). The estimated beam direction is shown as a thick black line. The wideband microphone is represented by a gray square, and was placed 0.3 meters above the floor. High-speed cameras are represented in diagram, and were positioned in the top corners of the room. The open room had an identical setup without artificial trees or side wall net.

Bats were trained in the open room. Once trained, a set of either 11 or 12 artificial trees as well as a net along one side of the room was introduced. The trees remained in the

same position for subsequent trials for each bat, however small changes to the tree positions occurred if the bats hit the trees during flight. Artificial trees were constructed using mist net (Avinet 38 mm mesh 75 denier/2-ply) wrapped around two metallic rings (diameter .254 m) connected vertically with strings (length 2.1 m) for support, creating a cylinder that was hung from the ceiling. The netting, stretched by the weight of the bottom ring, became narrower in the middle. The artificial trees were spaced approximately 1 m apart from their centers. A net connected the side wall of the flight room created a barrier to encourage the bats to explore within the forest and not to circle around the trees. Within the artificial forest, the tethered insect was hung in the space between trees. See Fig. 2.1 for schematic of experimental setup.

Table 2.1: Trials collected for each bat and day. Open and F1-F5 indicates the condition, either open room or forest day 1-5. Trial numbers are for both audio and trajectory analysis unless number in parenthesis present. Trial numbers in parentheses indicate the number of flight trajectory trials if different from the number of audio trials. These differences arose from problems in the wideband audio data collection.

Bat	*Open*	*F1*	*F2*	*F3*	*F4*	*F5*
B52	11	9	7	0	0	0
B52:Y2	4	10	6 (10)	10	10	10
B57	6	10	5	7	8	0
B57:Y2	5	5 (9)	0 (10)	10	10	10
B53	11	11	8	0 (9)	9	0
W50	14	16	0	0	0	0
O44	16	10	0	0	0	0
O40:Y2	0	7 (8)	7	0 (8)	6	6
B59:Y2	0	6	6	0 (6)	7	5 (7)

The number of trials for each bat is listed in Table 2.1. Note that two bats, O40:Y2 and B59:Y2, did not have open room data collected. Two other bats, B52 and B57 were

tested for a second year, so they were not naïve to the forest. However, these two bats experienced a different orientation of the trees in year two.

Experimental recording setup

Two high-speed cameras (Photron FASTCAM PCI R2) filmed the bats at 250 frames per second. We reconstructed the 3D flight paths using the direct linear transform algorithm with in-house software programmed in MATLAB and the KineMat toolbox (Reinschmidt & Bogert, 1997). A horizontally mounted microphone array (20 microphones) recorded the sound emission intensities of the bat vocalizations (for methods see: (Ghose & Moss, 2003). This allowed reconstruction of the horizontal beam pattern and calculation of the sonar beam axis. An ultrasound sensitive microphone (UltraSound Advice, SM2 microphone with SP2 amplifier) was used to record the wideband sonar emissions (bandpassed between the frequencies of 10 and 100 kHz, Wavetek-Rockland Dual Hi/Lo Filter) and recorded digitally (IoTech 512 Wavebook and computer). Data collection synchronization was achieved using a trigger switch connected to a TTL generator circuit that broadcast to each system. Each system was configured with an 8 second rolling buffer aligned to the onset of the TTL pulse. After each trial, data were downloaded.

Sound analysis

Sonar vocalizations on the wide-band recordings were processed using custom software written in MATLAB. Vocalization peak intensities were identified using the MATLAB findpeaks algorithm after squaring and smoothing the time-waveform and using a

threshold based on the noise of the recordings. Echoes were automatically ignored when the ratio between peaks differed by a magnitude of five or higher and the interval between pulse and echo was below 15 ms. Vocalizations were manually checked for echoes and skipped vocalizations. The call onsets and offsets were identified by using a recursive search for changes in energy. The sonar calls were either high-passed or low-passed (Butterworth filter, frequency cutoff at 30 kHz) for the onset and offset markings and were manually checked. Vocalizations with a PI below 10 ms (buzz phase) or with a signal-to-noise ratio that was too low did not have onsets or offsets marked and were excluded from duration analysis. Vocalizations with a PI above 300 ms were not included in analyses (determined to be either silent or missed prior vocalizations).

Sound groups were identified when their PI was less than 1.2 times the PI of surrounding vocalizations. For vocalizations occurring in groups of 3 or more, the PI differences between the vocalizations needed to be below 5%. Vocalizations outside the range of 10 to 100 ms were excluded.

Trajectory analysis

Flight speed was calculated over a smoothed flight trajectory to remove artifacts of 2D digitization (cubic spline interpolation over a sampled subset of the 2D camera data). The average turn rate was calculated as a three point moving average of the turn angle between each smoothed 3D position. Turn rates above 500 $^{\circ}$ s^{-1} (positioning errors) and turn rates of 0 $^{\circ}$ s^{-1} (stationary) were not included.

Occupancy histograms were created by collapsing the 3D trajectory data to 2D plan projection (*x,y*). The number of points across a set of flight paths were counted that fell inside 10 cm^2 bins. These points were converted to probabilities by dividing each bin count by the total number of points across each set of flights. After normalization, the occupancy histograms could be compared across days in forest. Bats with two or fewer days in the forest were excluded from trajectory comparisons over time (B52, W50 and O44).

Aim of sonar beam in relation to flight turn rate

We examined the correlation at time offsets -0.4 to 0.4 s. To obtain 95% confidence intervals for the correlation coefficient, *r*, we performed a Fisher transformation and calculated:

$$\pm z_{\alpha/2}\frac{1}{\sqrt{n-3}} \tag{2.1}$$

where $z_{\alpha/2}$ is 1.96 for 95% confidence intervals and *n* is the sample size. The confidence interval for τ_{max} was determined by considering the range of obtained *r* values not significantly different from the peak *r* value (±95% confidence interval). The data from three bats were combined for this analysis (B52, B57 and B53).

Temporal relationship between sonar vocalizations and flight trajectories

In this analysis, the distance to the nearest tree, independent of direction, was calculated for each call. Call emission times were set to the onset time (corrected for time of flight

to the microphone). For sound groups, the onset was the first vocalization of the sound group. All single sounds (non-sound group calls) were included except for calls with a PI below 10 ms. The distance between the bat and nearest tree was calculated along the trajectory between 100 ms to 300 ms after each vocalization. This range of time was used because it represented a portion of the trajectory that could be influenced by sonar echoes returning and because of the difference observed in distance to the tree along this interval. For each bat, an average across trials of the nearest tree distance was calculated for both sound group and single sound emissions.

Results

Performance

Nine wild, big brown bats were trained to catch tethered insects in an open laboratory room. Once bats reached proficiency at foraging in the open room, they were tested in an artificial forest (Fig. 2.1). While foraging, the bats were able to successfully maneuver without hitting trees (79% of trials with no crashes averaged across 9 bats, S.E.M: 6%). Although individual differences in the approach and flight trajectories existed, each bat was successful in the task.

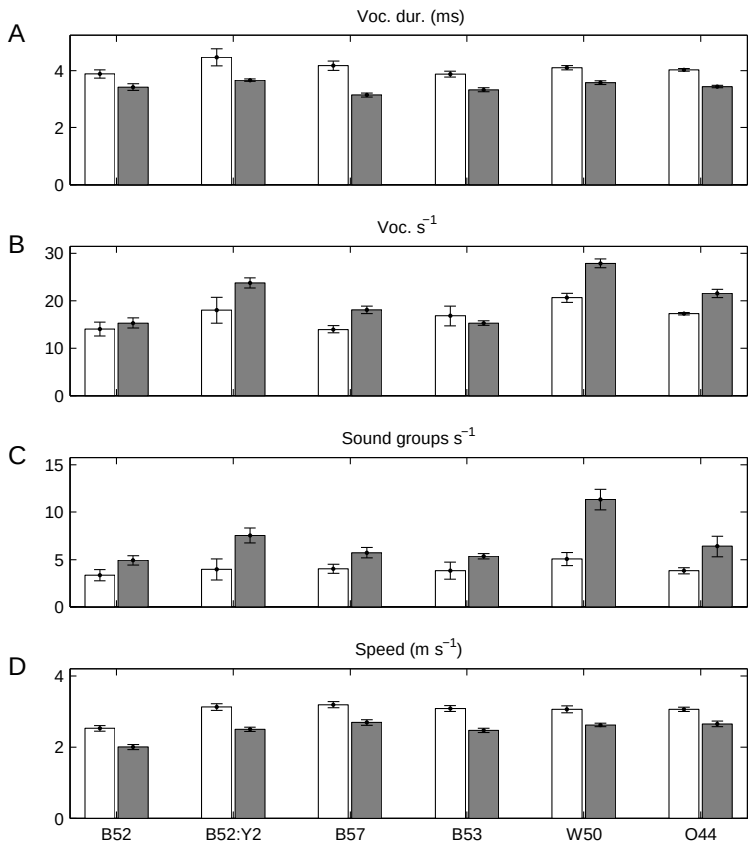

Fig. 2.2: Behavioral changes in big brown bats (*Eptesicus fuscus*) between open room and forest. Individual bat averages across trials for (A) vocalization duration excepting buzz calls, (B) vocalizations per second excepting buzz calls, (C) vocalizations in sound groups per second, and (D) flight speed for each bat. Results are means +/- s.e.m. White bars, open room recordings; gray bars, forest recordings.

Adaptive sonar and flight behavior

When foraging in the forest, the bats adapted the structure and temporal patterning of their sonar calls as well as their flight kinematics. We characterized these changes between the open room and the forest (Fig. 2.2, paired two-tailed t-test for each comparison). We found that bats in the forest emitted shorter duration vocalizations, mean 3.43 ms compared to 4.09 ms, $t(5) = 7.46$, $p < 0.001$, indicating that the bats

avoided pulse-echo overlap when flying near obstacles. The bats vocalized at a higher repetition rate in the forest, mean of 20.31 compared to 16.79 vocalizations per second, $t(5) = -2.73$, $p = 0.041$, which is indicative of sonar approach sequences but was also observed when bats were near obstacles. An increased repetition rate can increase the localizing resolution of sonar by providing more echoes from the surroundings. The bats not only increased the rate of calling, but also changed the temporal patterning of their vocalizations when in the forest. The bats emitted a higher rate of sound-group vocalizations – clusters of closely spaced emitted calls – in the forest, with a mean of 6.87 compared to 4.00 sound groups per second in the open room, $t(5) = -3.80$, $p = 0.013$. Bats flew at slower speeds in the forest than in the open room, mean of 2.49 m s^{-1} compared to 3.01 m s^{-1}, $t(5) = 14.22$, $p < 0.001$, which is consistent with bats flying between obstacles. A decrease in flight speed allowed bats additional time to react to obstacles and maneuver through the forest.

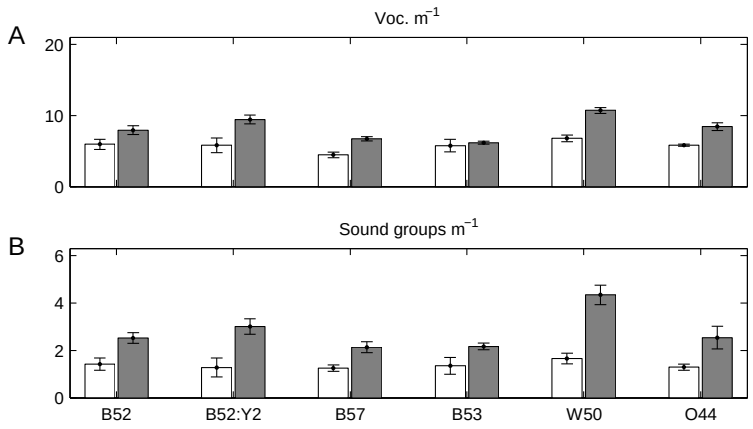

Fig. 2.3: Sonar behavior in relation to distance traveled in big brown bats. Individual bat averages across trials for (A) pulse density, or number of vocalizations per m traveled, and (B) sound group density, or number of sound group vocalizations per m traveled. Results are means +/- s.e.m. White bars, open room recordings; gray bars, forest recordings.

The decrease in flight speed in the forest also served to increase the pulse density, or the number of vocalizations emitted per meter traveled, with a mean of 8.25 vocalizations per meter in the forest compared to 5.77 in the open room, $t(5) = -4.80$, $p = 0.005$. The sound group density also increased in the forest, with a mean of 2.79 sound group vocalizations emitted per meter traveled compared to 1.38 in the open room, $t(5) = -4.91$, $p = 0.004$ (Fig. 2.3). An increase in pulse density and sound group density increased the information flow by increasing the number of echoes returning from obstacles as the bats navigated the artificial forest.

Steering by hearing in the forest

A bat's sonar gaze angle (beam aim relative to flight direction) has been found to be linked to its flight motor output through a delayed linear model (Ghose & Moss, 2006). The general control law was defined as the linear relationship:

$$\dot{\theta}_{flight}(t+\tau) = k\,\theta_{gaze}(t) \tag{2.2}$$

where θ_{gaze} is the gaze angle (the angle between the beam axis and flight vector), $\dot{\theta}_{flight}$ is the rate at which the bat turns, k is a state-dependent gain factor, and τ is the constant time by which the flight lags the gaze direction. In the original study (Ghose & Moss, 2006), this linear relationship varied depending on the phase of the sonar sequence (search, approach, or buzz or terminal phase). We examined whether a change in environment could alter the link between sonar acoustic gaze and turn rate.

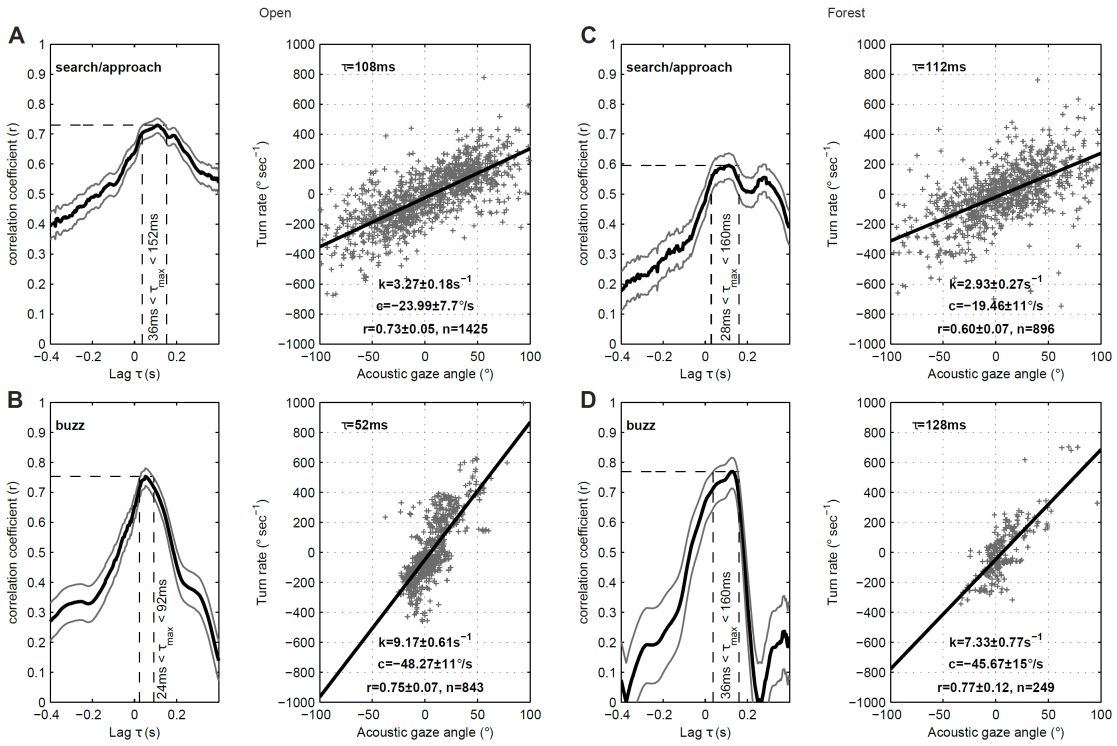

Fig. 2.4: Sonar beam direction and turn rate correlation analysis between open room and forest during search/approach and buzz phases of echolocation. Open room (A, B) and forest (C, D) and search/approach (A, C) and buzz (B, D). Left panels show calculated correlation, *r* (black line, C.I. in gray), between acoustic gaze angle and turn rate for time lags, -0.4 to 0.4 s. The peak correlation, found at τ_{max}, is indicated with a dashed horizontal line. C.I. for τ_{max} is indicated with dashed vertical lines. Right panels show the linear correlation at τ_{max}. The gaze angle and corresponding turn rate are plotted (gray crosshairs). The fitted linear relationship plotted in black. *k* refers to the slope of the fitted line, *c* refers to the intercept, *r* is the correlation, and *n* is the number of vocalizations.

Table 2.2: Relationship between acoustic gaze angle and turn rate for open room and forest in search/approach and buzz echolocation behavior. The peak correlation (r), the delay at the peak (τ_{max}), gain (k) at τ_{max}, and the number of vocalizations (n). Values for r and k are means +/- 95% confidence intervals.

	τ_{max}	*CI*	r	k	n
Search/Approach, Open	108	36 – 152	0.73 ± 0.05	3.27 ± 0.18 s^{-1}	1425
Search/Approach, Forest	112	28 – 160	0.60 ± 0.07	2.93 ± 0.27 s^{-1}	896
Buzz, Open	52	24 – 92	0.75 ± 0.07	9.17 ± 0.61 s^{-1}	843
Buzz, Forest	128	36 – 160	0.77 ± 0.12	7.33 ± 0.77 s^{-1}	249

A linear relationship between acoustic gaze and flight turn rate was determined for search/approach (PI > 20 ms) and buzz (PI < 10 ms) phases of the sonar sequence (Fig. 2.4). The correlation, *r,* was found for different time delays, *τ,* relative to each vocalization. The maximum correlation, τ_{max}, was compared between open room and forest for search/approach and buzz echolocation phases (Table 2.2). Late approach phase vocalizations (PI between 10 and 20 ms) were not well represented in the present dataset (6% of vocalizations in the open room and 4% in the forest) and were excluded from this analysis. No statistical differences between the values of τ_{max} were found, however all were significantly above zero (Table 2.2).

The linear model at τ_{max} was examined for open room and forest and across the phases of echolocation sequence (ANCOVA). Pairwise comparisons of the gain, or slope, of the linear relationship showed a larger gain in the buzz phase than in the search/approach phase (Table 2.2). This result is consistent with the finding in (Ghose & Moss, 2006) in the open room alone. The gain was larger in the open room than in the forest during the sonar buzz phase (Bonferroni correction, Table 2.2). The larger gain in the open room

during the buzz phase coincided with an overall decrease in turn rate in the forest during buzz phase (two-sample t-test, $t(904) = 3.57$, $p < .001$) with no change gaze angle ($t(904) = 0.42$, $p = .67$). These findings indicate that the environment shapes the relationship between gaze angle and flight motor output.

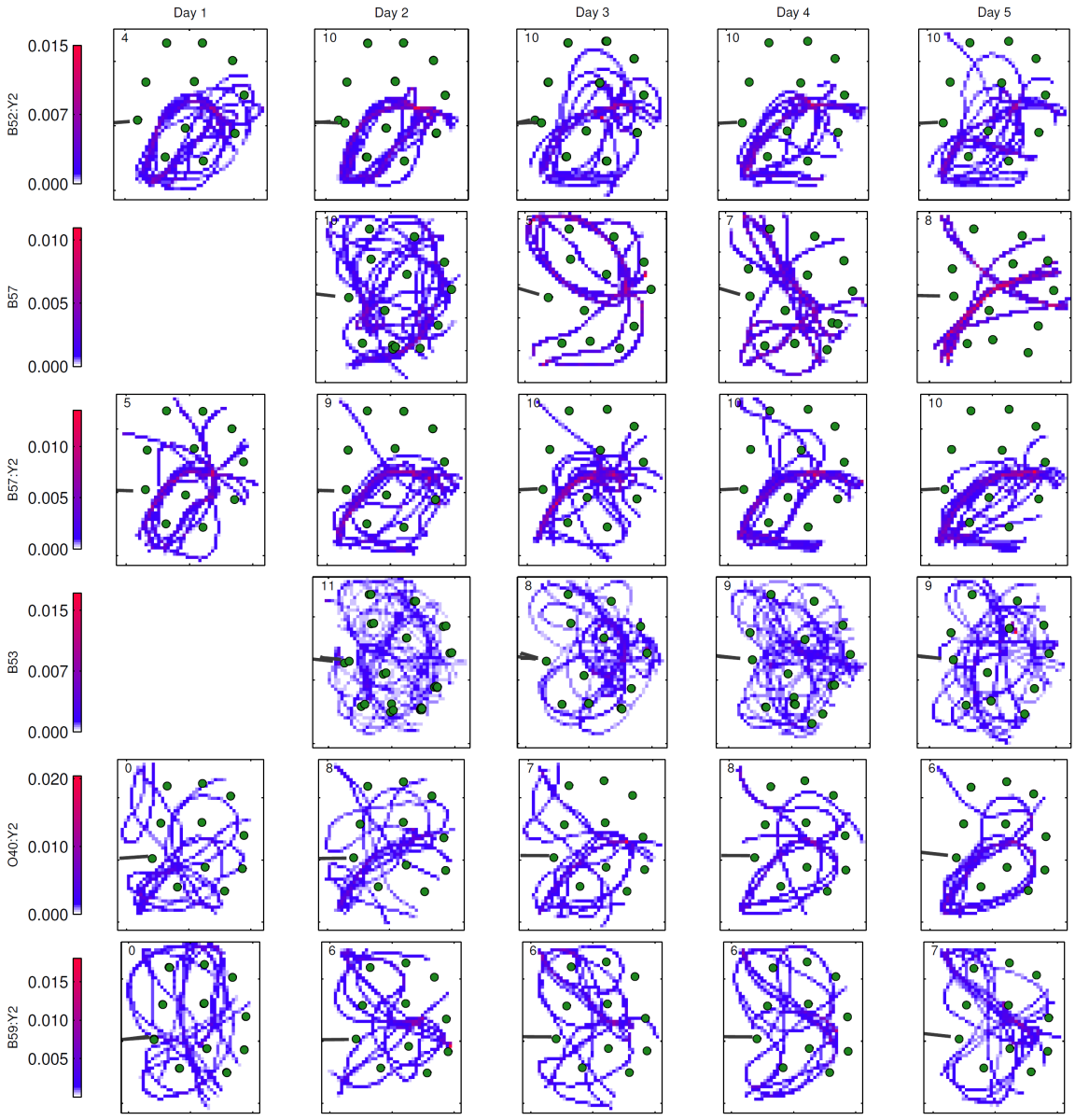

Fig. 2.5: Trajectory-occupancy histograms for each bat and day represented as heat map in top view. Tree positions for each trial overlaid on top of each other, represented as green circles. Occupancy as a percentage of time is shown by change in color from white to blue to red (indicated in scale on left), in order of least likely to most likely to occur. Number of trials per day is shown in top left corner of each panel.

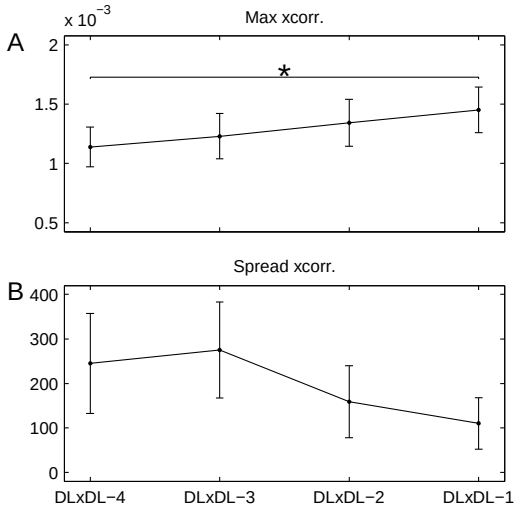

Fig. 2.6: Measures of cross correlation of occupancy histogram of last day in forest with each previous day in forest. Along x-axis, DL indicates last day in the forest for each bat. The cross correlation day is relative to the last day in the forest, between 1 and 4 days before the last day (DL-1 through DL-4). (A) Maximum (peak) of each cross correlation. (B) Spread (# of points above 60% of the maximum) of each cross correlation. These values were averaged across bats and plotted as the means +/- the s.e.m. The only significant change (P=0.002) is shown with the asterisk and labeled line between the cross correlation with DL-4 and DL-1 for the maximum cross correlation.

Spatial memory vs. active sensing

Stereotyped flight paths which develop over time indicate that bats are relying on their spatial memory, and they have been found to coincide with a reduction in active sensing in non-foraging bats navigating obstacles (Barchi et al., 2013). We tested foraging bats in the artificial forest for these effects over several days (see Table 2.1 for number of trials collected). We calculated 2D occupancy histograms from bat flight trajectories (Fig. 2.5) and cross correlated the occupancy histograms of the last day in the forest with each previous day for each bat. We calculated the peak (maximum) and spread (number of points above 60% of the maximum) of each cross correlation for each bat to measure the

development of flight stereotypy over time (Fig. 2.6). A repeated measures ANOVA for both the peak and the spread of the cross correlations resulted in a statistically significant change in peak ($F(9) = 11.12$, $p = .002$) but not spread ($F(9) = 2.12$, $p = .17$). A pairwise comparison on the peak found an increase between the first and last cross correlation (difference 3.13×10^{-04}, $p = .02$, Holm-Bonferroni adjustment), indicating that flight patterns became more similar between the first and last day in the forest.

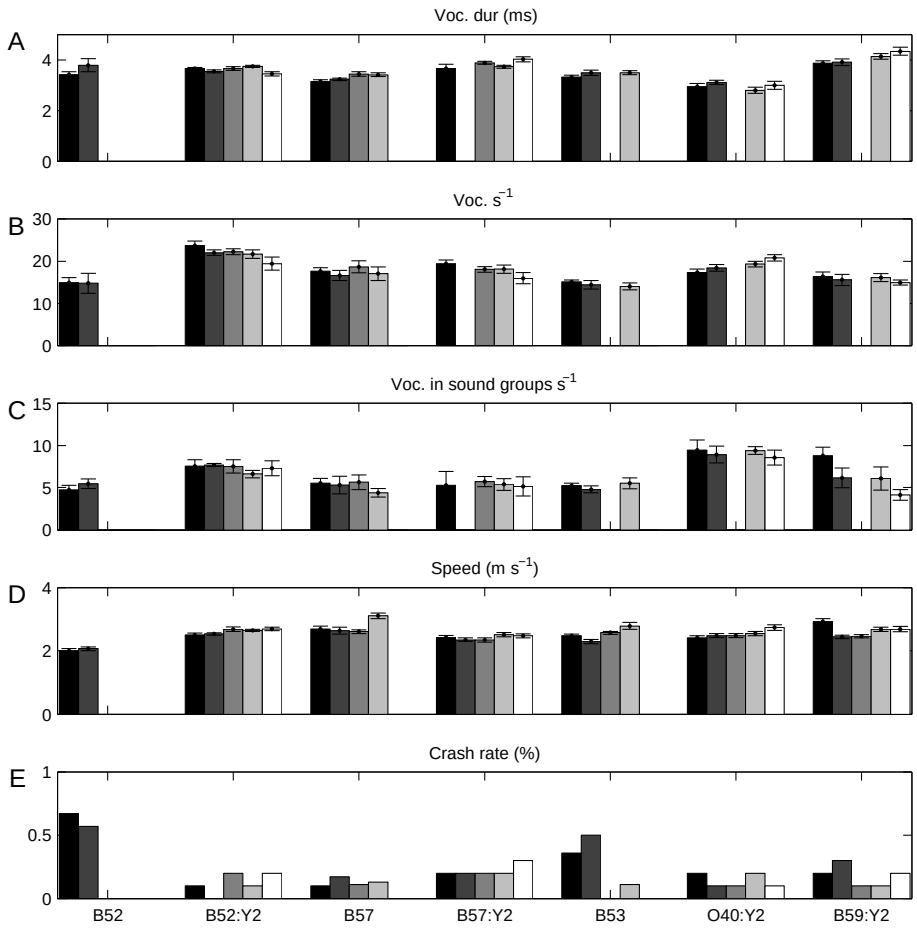

Fig. 2.7: Sonar and flight behavior over time in forest. Data for forest day 1 to forest day 5 are indicated by gradation in color from black to white (left to right) for each bat. Trial averages for (A) vocalization duration, (B) vocalizations per second, (C) vocalizations in sound groups per second, and (D) flight speed. Values shown are means +/- s.e.m. (E) Crash rate as a percentage of flights per day. Gaps in between data points in sonar data for bats B57:Y2, B53, O40:Y2, B59:Y2 in A-C due to absent microphone data. Bats had up to 5 days of flight in the forest but some had fewer (see Table 2.1).

We then investigated whether bats altered their active sensing or flight kinematics over time in the forest by measuring vocalization duration, number of emitted vocalizations per second, sound groups vocalizations emitted per second, and flight speed. We found no evidence for changes over successive days in the forest (Fig. 2.7A-D). Similarly, we

found no changes in the crash rate over time in the forest (Fig. 2.7E). These findings indicate that the bats did not rely on spatial memory in place of active sensing.

Path planning and sonar temporal patterning

Bats use a complex sampling strategy when foraging in the forest; the spatial locations and temporal patterning of the emitted sonar calls are both varied and systematic. Bats emitted sonar sound groups while navigating the forest, often at high rates (see Fig. 2.2). Sound groups may provide additional spatial resolution for localization of nearby objects. The temporal patterning of the emitted sonar calls and their relation to objects in the room along with each bat's movement through space was further investigated.

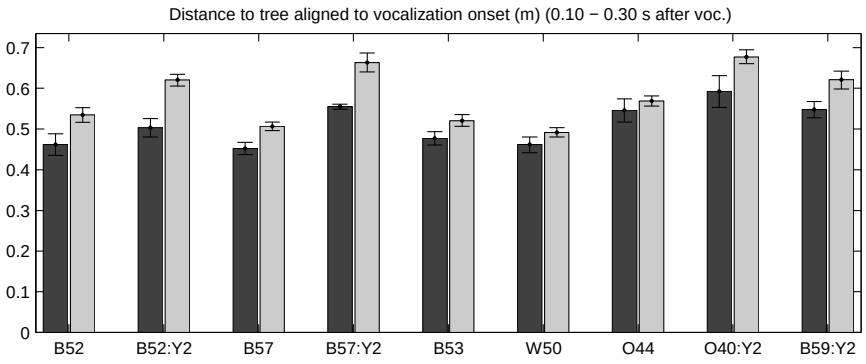

Fig. 2.8: Time-aligned distance to nearest tree for sound group vocalizations compared with single sound vocalizations. Bat averages across trials for distance to tree aligned to vocalization onset is shown (0.1-0.3 s after vocalization). Sound groups distances are in black; single-sound distances are gray. Error bars are s.e.m.

We examined the relationship between the temporal patterning of sonar calls and the resulting flight path navigation. We calculated the distance from the bat to the nearest

tree and time aligned the resulting distance to the sonar sound groups or single vocal emissions. Between a period of 100-300 ms after the onset of vocalization, bats were closer to the nearest tree for sound group emissions than single call emissions (Fig. 2.8, two tailed two sample t-test, mean of 0.51 m for strobe calls compared to 0.58 m, $t(16) = -2.35$, $p = 0.032$). The average duration of a complete sound group (onset of first call to onset of last call) for bats in this study was 106 ms for doublets (82% of sound groups) and 136 ms for triplets (15% of sound groups). These results indicate that bats navigating the forest use sonar sound groups before approaching the trees.

Discussion

Bats foraging in different environments face a variety of challenges, from target detection to figure ground segregation. Here, we find that this bat species adapts sonar and flight behavior in concert when shifting from open to cluttered environments.

Adaptive behavior to obstacles

We found that big brown bats shortened their sonar signal duration and increased their repetition rate in the artificial forest compared with the open room (Fig. 2.2A, B). Shortening the sonar signal duration decreases pulse-echo overlap (Kalko & Schnitzler, 1989, 1993), which allows a bat to more easily process echoes from closely spaced objects. Higher sonar signal repetition rate increases the rate of echo sampling of the environment. Both of these echolocation adaptations may have served to increase localization accuracy for the bats as they navigated the artificial forest in this study.

Our data point to a potential link between sound groups and flight path planning. The bats in the present study increased the rate of emitted sound groups in the forest (Fig. 2.2C). An increase in sound group production has been reported when bats encounter clutter or nearby obstacles (Moss et al., 2006; Moss & Surlykke, 2001; Petrites et al., 2009; Sändig et al., 2014). We found that when bats emitted sonar sound groups in the forest, they were closer to trees between 100 and 300 ms after vocalization emission time, compared to when they produced single calls (Fig. 2.8), indicating that the bats organized calls into groups when they were preparing to approach artificial trees. On average, each sound group was completed (including echo arrival time) before the bats reached the closest distance to a tree. Sound groups often occur at a different phase of the wing beat than single calls (Moss et al., 2006), and the timing of the sound group, in relation to wing beat, is probably planned prior to the sound group initiation (Koblitz et al., 2010). The delay between emitted sound group and resulting trajectory distance to a tree allows for sonar ranging before nearing obstacles and for path planning. Therefore, production of sound groups seems to be involved in path planning around obstacles.

We observed that bats flew slower in the forest (Fig. 2.2D). Studies on other species of bats and birds have found that slow flight incurs significant energetic costs (Norberg, 1990; Thomas, 1975). Wing morphology measures of aspect ratio for *E. fuscus* (Farney & Fleharty, 1969) indicates that this species is not well adapted for slow flight and that energetic costs would be higher when flying at slow speeds. However, by flying slower, the bats can more easily maneuver around obstacles without crashing. Slower flight,

together with the changes in sonar behavior in the forest, resulted in an increase in pulse density and sound group density, which provided additional echo information for localizing obstacles. Slow flight also provided time for processing echoes and path planning. Slow flight in the forest served multiple functions, affecting both flight maneuverability and biosonar performance.

Linking between acoustic gaze and flight motor output

Ghose and Moss (2006), studying bats foraging in an open room, reported a linear relationship between gaze angle and a positively delayed turn rate. In our experiment, we compared this relationship in both the open room and the forest (Fig. 2.4). A cluttered environment might alter this relationship, as the bats need to respond to nearby obstacles quickly, the flight motor output may rely more on spatial memory instead of sonar, reducing the time lag or even making it negative. However, we found that the lag time that produced the maximum correlation was positive in the forest as well as the open room, confirming that the bats' acoustic gaze leads flight motor output, even in a cluttered environment.

Ghose & Moss (2006) also found that the gain, or slope, in the linear correlation between gaze angle and turn rate, was higher in the sonar buzz phase than the search/approach phase. We found a similar increase in gain between the buzz phase and search/approach phase, regardless of environmental condition. This result suggests that the behavioral state of the animal has a strong influence on the link between gaze angle and turn rate. In this analysis, we compared the gain between the open room and the forest and found a

decrease in the sonar buzz phase in the forest, as well as an overall decrease in turn rate in the forest during buzz phase. The shallower turn rate during buzz phase in the forest was not observed during search/approach phase. These findings highlight the important interaction between flight kinematics and sonar behavior. The gain of the relationship between gaze angle and turn rate depends on both the flight and sonar gaze, which are modified by the behavioral state of the animal, as well as the complexity of the environment.

The slope relating gaze angle and turn rate in the open room in our experiment was found to be higher than reported in Ghose & Moss (2006) for the buzz phase. In addition, the percentage of late approach (tracking) phase vocalizations was found to be lower in our experiment than that reported previously Ghose & Moss (2006). The Ghose and Moss study was conducted in an open room but the tethered insect was dropped from a trap door towards the end of the trial instead of remaining stationary tethered from the ceiling. The certainty in the insect position in our experiment may have decreased late approach phase vocalizations and also decreased acoustic gaze angle. A lower gaze angle could lead to the higher gain reported in our study.

Spatial memory vs. active sensing

We did not find any changes in the sonar behavior as the bats gained experience in the forest, indicating that the bats in our study relied more on active sensing than on spatial memory (Fig. 2.7). However, we did find an increase in flight path stereotypy over days (Fig. 2.6). (Barchi et al., 2013) examined spatial memory with bats flying through a

chain array and found a strong effect of stereotypy as well as a decrease in vocal repetition rate over time. However, in the (Barchi et al., 2013) study, the bats were not foraging. We suspect that foraging places demands on bats that limit their use of spatial memory, because flight paths in the present study were more variable than those reported for bats navigating obstacles in the absence of prey (Barchi et al., 2013). Foraging requires accurate localization of obstacles and prey, and requires precise planning of complex flight motor behaviors in order to capture the prey item. These requirements likely force bats into a continuous active sensing mode, and reduce their reliance on spatial memory.

A bat's representation of its environment is built upon its sonar system that processes echo information over time. In order for bats to successfully fly at high speeds, within a complex, cluttered environment, bats must continuously update their perception of space. Bats can rely on spatial memory for navigation, sometimes in place of active sensing (Barchi et al., 2013; Jensen, Moss, & Surlykke, 2005), but in the present study, we find that requirements in path planning, object localization, and foraging maneuvers require continuous active sensing. Bats in the present study were actively foraging and the results point to the importance of continuous sonar updates, in contrast to situations of "transport" flight, where memory may take over in well-known surroundings.

Active perception is guided by action in a task-driven manner. However, motor behaviors subsequently propagate backwards to dictate scene sampling. Here, we sought to understand the motor actions driving the acquisition of information for scene analysis.

This study links the animal's acoustic input and motor output to uncover adaptive active sensing behaviors, which depend on both the behavioral state of the animal and the environment.

Acknowledgments

We would like to thank Ninad Kothari for comments on an earlier version of the manuscript.

Chapter 3 is in review as:

Tight coordination of aerial flight maneuvers and sonar call production in insectivorous bats

Benjamin Falk, Joseph Kasnadi, Cynthia F. Moss
(in review). The Journal of Experimental Biology.

Chapter 3: Tight coordination of aerial flight maneuvers and sonar call production in insectivorous bats

Abstract

Echolocating bats face the challenge of coordinating flight kinematics with the production of echolocation signals used to guide navigation. Previous studies have focused on flight performance of fruit and nectar feeding bats, often in wind tunnels with limited maneuvering. In this study, we engaged insectivorous big brown bats in a task requiring simultaneous turning and climbing flight, and used synchronized high-speed motion tracking cameras and audio recordings to quantify the animals' coordination of wing kinematics and echolocation. Bats varied flight speed, turn rate, climb rate, and wingbeat rate as they navigated around obstacles, and they adapted their sonar signals in patterning, duration, and frequency in relation to the timing of flight maneuvers. We found that bats timed the emission of sonar calls with the phase of the wingbeat in straight flight, and that this relationship changed while turning to navigate obstacles. We also characterized the unsteadiness of climbing and turning flight, as well as the relationship between speed and kinematic parameters. Adaptations in the bats' echolocation call frequency suggest changes in beam width and sonar field of view in relation to obstacles and flight behavior. By characterizing flight and sonar behaviors in an insectivorous bat species, we find evidence for exquisitely tight coordination of sensory and motor systems for obstacle navigation and insect capture.

Introduction

Insectivorous bats make agile flight maneuvers in the dark to navigate around obstacles and intercept prey. Bats adapt wing kinematics, including adjustments in wing camber, wing area, angle of attack, and the rotation of the wing, in order to achieve maneuverable flight across different speeds and generate appropriate lift, thrust, and vortex flow (Aldridge, 1986; Hubel et al., 2012; Norberg, 1976b; Norberg & Winter, 2006; Riskin et al., 2008; Tian et al., 2006). Flapping flight allows rapid changes to aerodynamic forces, which is important for maneuverability. The generation of a leading edge vortex, a time-varying unsteady mechanism, increases lift during slow, hovering flight (Hedenström et al., 2007; Muijres et al., 2008, 2014). While many studies on bat flight have focused on straight or hovering flight, maneuvering, climbing, and turning flight have not been as systematically investigated, where unsteady effects may be more pronounced. In the present study, we examine how the dynamics of flapping flight interact with the timing and performance of the bat's sonar guidance system.

Echolocating bats emit sonar signals and process information carried by returning echoes to localize objects in their environment (Griffin, 1958). Open-space insectivorous bats emit high intensity calls, which can exceed 135 dB SPL at 10 cm (Holderied et al., 2005; Surlykke & Kalko, 2008). To maximize energy efficiency, bats often time the sonar call production to occur during exhalation, which coincides with the upstroke of the wingbeat cycle (Schnitzler, 1971; Suthers, Thomas, & Suthers, 1972). In addition, periods of silence, when pulses are not produced, primarily occur during inspiration along the downstroke of the wingbeat (Wilson & Moss, 2004). However, the relationship between

sound production and respiration is not fixed; sounds can be produced throughout the wingbeat cycle (Moss et al., 2006), with sound intensity varying with the wingbeat (Koblitz et al., 2010). Variation in bat call intensity and timing with respect to wingbeat cycle indicates that task demands impart tradeoffs between energy efficiency in vocal production and sonar information acquisition.

Bats adjust the timing of sonar sounds as they operate in different environments or perform different tasks. When searching for food in open space, big brown bats emit sounds at a slow rate of 5-10 Hz (Griffin, 1958; Surlykke & Moss, 2000). When they near an insect or fly amidst clutter, they increase the rate of sound production, augmenting the rate of echo information updates per unit time (Moss & Surlykke, 2001). As bats capture an insect or prepare to land, they emit a terminal buzz, in which sounds are produced at a rate as high as 200 Hz, which is about 20 times the rate of the big brown bat's wingbeat cycle. Bats also emit groupings of sounds, which occur closely spaced in time and show the following relationship to the wingbeat cycle: first calls in a group occur earlier in the wingbeat cycle, last calls in a group occur later in the wingbeat cycle, and the group as a whole is centered around the peak of the upstroke, where single calls also occur (Koblitz et al., 2010). The temporal patterning of the group appears to be set by the emission time of the first call in the group, relative to the wingbeat, and indicates that the emission pattern of a sound group is pre-planned. The variable timing of sonar call production with respect to wingbeat allows the bat to adapt to different environments and task requirements.

Insectivorous bats emitting frequency-modulated (FM) calls also adapt the duration, frequency, intensity and directionality of their sonar calls. Bats reduce call duration to avoid pulse-echo overlap with nearby objects (Cahlander et al., 1964; Kalko & Schnitzler, 1989; Schnitzler et al., 1987), widen call bandwidth to better localize objects (Faure & Barclay, 1994; Hartley, 1992; Kalko & Schnitzler, 1993; Surlykke et al., 1993), reduce call intensity as they approach objects as a method for keeping target echo strength constant (Hartley, 1992; Hiryu et al., 2007), and decrease directionality to widen the field of view as they attack prey (Jakobsen & Surlykke, 2010). These signal adaptations occur as the bat adjusts the timing of sonar sounds, and may also be influenced by the temporal dynamics of respiration and flight kinematics.

In this study, we examined flight motor output with the relative timing of sonar vocalizations to better understand the coordination of flight kinematics and sonar behavior. We tested big brown bats, *Eptesicus fuscus*, in a challenging flight task in which the animals were required to make two sharp turns and a steep climb in order to capture a tethered insect. We investigated flight and echolocation systems as drivers for coordinated behaviors and examined fine scale changes to call production as bats navigated a complex environment.

Materials and Methods

Five adult, wild-caught big brown bats, *Eptesicus fuscus,* Palisot de Beauvois, 1796, were trained to participate in these studies and complete data sets were collected from three of these animals. *E. fuscus* forages in open spaces as well as clutter (J. A. Simmons et al.,

2001) and has a highly variable and adaptive sonar system. Experiments took place in a large flight room (7.5 x 6 x 2.5 m) at the University of Maryland, College Park, in low light conditions and lined with sound absorbing foam (Sonex One, Acoustical Solutions, Inc.). All experimental procedures were approved by the Institutional Animal Care and Use Committee at the University of Maryland, College Park.

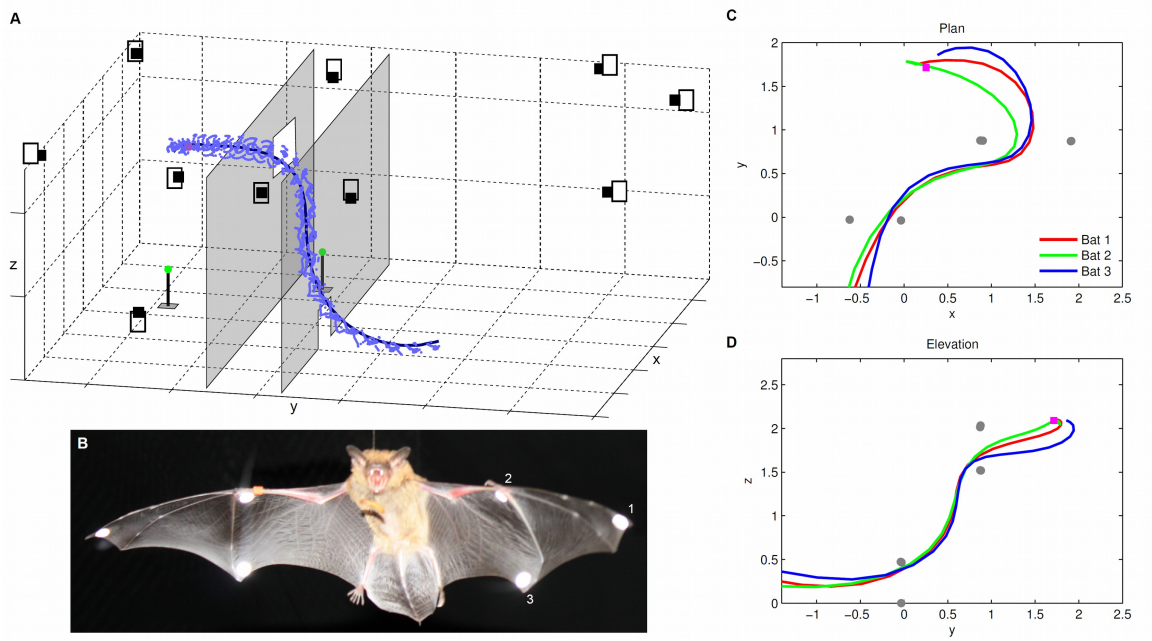

Fig. 3.1: Schematic of flight room with example trajectory, reflective marker locations on the wing, and plan and elevation views of averaged trajectories. (A) Ten motion tracking cameras (black and white rectangles) appear around the room with approximate camera aim indicated. Reflective markers on the wings of the bat return reflections to the camera system which turns them into 3D coordinates (light blue). A smoothed centroid calculated from the positions of the markers (dark blue) represents the bat's trajectory through the flight room. Two nets (gray) with openings separate the room. The first net, on the right of the schematic, has an opening near the floor while the second net, on the left, has an opening near the ceiling. Ultrasound-sensitive microphones were mounted on the floor (green circles) and the tethered insect was placed after the second net (magenta-colored circle). 3D positions of the objects in this schematic were extracted from the motion tracking camera system. (B) Photo of the bat in flight during capture of tethered insect in which reflective markers are visible on the ventral side of the wing. Markers were placed at the wing tip (1), near the thumb joint (2), and at the base of the wing near digit five (3). Markers on the dorsal side of the wing are present but not visible in this photo. (C & D) Data were aligned in time to the first net crossing and 3D positions were averaged along 0.1 second time bins. Bats 1, 2, and 3 plotted in red, green and blue lines. Net opening corner positions plotted as gray circles. The tethered insect position is shown as a magenta square. Plotted as plan projection (C) or elevation projection (D).

Experimental setup

Over a period of two months, bats were trained to fly though a corridor created with two parallel nets, spaced 0.9 m apart. The nets had two small openings, which served as an entrance and exit to the corridor (deer block netting, PVC mesh, 1.5 cm x 1.5 cm holes). The nets spanned the height and width of the flight room (Fig. 3.1, top panel). The first net opening (area 0.27 m^2) was placed close to the ground on one side of the room, while the other net opening (area 0.51 m^2) was placed close to the ceiling on the other side of the room. The bats were trained to catch insects (*Tenebrio molitor* larvae) tethered and hanging from the ceiling by monofilament fishing line (Berkley Trilene, 0.9 kg test, 0.13 mm diameter). The tethered insect was hung 0.76 m behind the second net and towards the middle of the room. This setup required the animals to navigate through the lower net opening, ascend and turn through the corridor, navigate through the second net opening, turn towards the tethered insect, and finally make insect capture.

Data recordings

We recorded 94 animal flight trials for each bat over a period of four consecutive days. Two ultrasound sensitive microphones (UltraSound Advice, SM2 microphone with SP2 amplifier) were used to record the wideband sonar emissions (band-passed between the frequencies of 10 and 100 kHz, Wavetek-Rockland Dual Hi/Lo Filter) and recorded digitally (National Instruments PCI-6122, sampling rate 250 kHz). A set of ten motion tracking cameras (Vicon MX T40) tracked reflective markers placed on the bats at 300 Hz. Motion tracking data was downloaded to a computer running Vicon Nexus software and exported to MATLAB (Mathworks) for further analysis. A set of markers, reflective

tape cut into 6.35 mm diameter circles, were attached to the wings of the bats. On each wing, markers were placed at the thumb joint, the base of the wing near digit five, and at the wing tip on both the dorsal and ventral sides (Fig. 3.1, bottom panel). Markers were fixed to the bat using tape adhesive and were replaced each day if any fell off. A hemispherical marker was also attached to the body but was rarely visible for motion tracking and was not used in analysis. Data synchronization was achieved using a trigger switch that broadcast a TTL signal to each system. Each system was configured with an 8 second rolling buffer aligned to the onset of the TTL pulse.

Trials in which the bats did not fly directly between the first net opening and the second net opening (indirect flight) were excluded from analysis. These trials were excluded if the time to cross the nets was larger than one standard deviation above the median time and if the flight speed was below 2 standard deviations of the median speed. We also did not analyze a set of trials in which there were tracking problems, reducing the total number of trials from 94 for each bat to 86, 85, and 78 for bats 1, 2 and 3, respectively. Direct flights comprised 81.4%, 81.2%, and 75.6% of trials for bats 1, 2, and 3, resulting in 70, 69, and 59 trials analyzed per bat.

Sound analysis

Recordings of sonar vocalizations were analyzed using custom software written in MATLAB. Vocalization peak intensities were identified from a squared and smoothed (200 point moving average) version of the time-waveform using the MATLAB findpeaks function with a threshold which adapted to the noise floor of each recording. Echoes

were automatically excluded when the ratio between peaks differed by a magnitude of five or higher and the interval between pulse and echo was below 15 ms. The waveforms and spectrograms of the vocalizations were visually inspected for accurate inclusion in the data set.

The call onsets and offsets were identified using a custom made function which searched for changes in energy. The sonar calls were high-passed, for onset markings, or low-passed, for offset markings (Butterworth filter, frequency cutoff at 30 kHz for both). Vocalizations with a PI below 10 ms (terminal buzz phase) or with low signal/noise (adapted to the noise floor of each recording and the intensity of the previous call) did not have onsets or offsets marked and were excluded from duration analysis. We visually inspected and corrected the markings on spectrograms. The onsets and offsets were used to calculate call duration values.

The end frequency of each frequency-modulated (FM) sonar call was automatically extracted from the last half of each call. A squared, smoothed frequency spectrum was calculated (smoothing: 20 point moving average). Values outside 10-40 kHz were ignored in order to suppress harmonics, echoes, and background noise. The end frequency was determined by an adaptive amplitude threshold crossing on the squared, smoothed spectrum values. Each frequency marking was visually verified using spectrogram plots.

Sound groups were identified as clusters of sounds, surrounded by calls with larger intervals (PI > 1.2 times the mean interval of the sound group). For call pairs, or doublets, the variation in PI is not relevant and not used as a means for inclusion, but for three or more sounds, call groups were characterized by the additional criterion of stable PI (< 5% variation). Vocalizations occurring with pulse intervals outside the range of 10-100 ms were not examined for sound group inclusion. The methods for identifying sound groups are the same as used by (Moss et al., 2006). Sound groups with three calls present were termed triplets.

Echolocating bats that use FM sonar signals reduce call duration with object distance to avoid pulse-echo overlap (Kalko & Schnitzler, 1989). We calculated the pulse-echo overlap zone (Kalko & Schnitzler, 1993), also referred to as inner window (Wilson & Moss, 2004), which is the boundary at which echolocation calls of a given duration would overlap with echoes arriving at a given delay and is defined as:

$$\frac{d * c}{2} \tag{3.1}$$

where d is the sonar pulse duration, c is the speed of sound (we used a constant 344 meters per second), and dividing by two accounts for the two way travel time of the pulse.

Flight path analysis

Motion tracking data was used for flight trajectory analysis. For each frame, we calculated a centroid from the recorded reflections of the markers on the bats. We

smoothed this centroid data using a 60 point moving average weighted by the number of reflections recorded within each frame. After smoothing, small gaps in the trajectories, due to missing reflections, were spline filled. Wingbeat oscillations were removed when calculating speed, turn rate, and climb rate using a low-pass Butterworth filter (cutoff frequency 6 Hz, order 6 with zero phase). The instantaneous speed of the bat was calculated as the distance traveled by the bat between each frame. The instantaneous turn rate was calculated as the difference in angular flight direction, along the x/y plan projection between each frame, and smoothed using a 60 point moving average. The instantaneous climb rate was calculated as the difference in elevation between each frame.

For wingbeat calculations, the original unfiltered centroid data was filtered with a 15 point moving average, weighted by the number of reflections recorded within each frame. The altitude values in this smoothed centroid were band-passed (Butterworth filter, cutoff frequencies 6 and 20 Hz, order 12 with zero phase) in order to isolate wingbeat oscillations. We determined the locations of the wingbeat peaks and troughs using the findpeaks MATLAB function. An instantaneous phase of the wingbeat was calculated from the analytic signal (Hilbert transform of the smoothed and band-pass filtered altitude data) and was used for aligning the vocalization times to the phase of the wingbeat. For calculating the mean wingbeat cycle angle of vocalizations with confidence intervals we used the 'CircStat Toolbox for MATLAB' (Berens, 2009).

Results

Three bats completed a series of 94 trials each, over four test days, flying to a food reward through a corridor created with a pair of parallel nets spanning the width of the experimental test room (Fig. 3.1A). In each trial, the bat entered the corridor through an opening low to the ground, climbed to the end of the corridor, where it flew through a second net opening close to the ceiling, and then captured a tethered insect (Fig. 3.1C, D). We analyzed trials in which the bat flew directly between the two net openings, resulting in 70, 69, and 59 trials per bat.

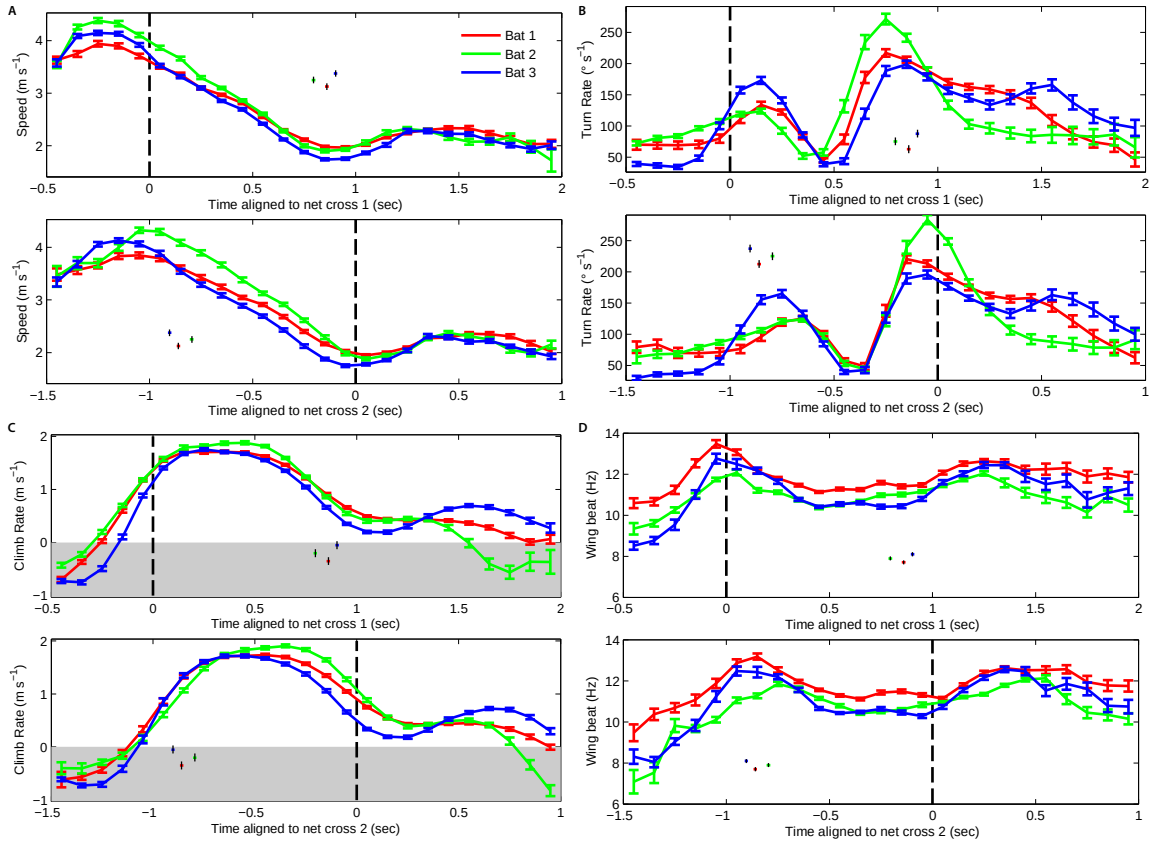

Fig. 3.2: Average flight measures across trials for each bat relative to net crossings. (A) Flight speed (meters per second), (B) turn rate (degrees per second), (C) climb rate (meters per second), and (D) wingbeat rate (Hz). Across each measure, the top panel is aligned to the first net crossing and the bottom panel is aligned to the second net crossing. Data were averaged across trials along 0.1 second time bins. Bat 1 in red, 2 in green, and 3 in blue. Values plotted are means +/- s.e.m. The aligned net crossing is shown at zero seconds with a dashed black line. The average net cross time of the other net crossing is represented as a short vertical line (black) with the s.e.m. represented as a horizontal line (color coded to each bat). In (C) the shaded region is negative climb-rate (diving).

Table 3.1: Flight behavior measures of the bats crossing between the nets. Values are means +/- s.e.m.

Bat	**1**	**2**	**3**	***Mean***
Number of trials	70	69	59	
Time (sec)	0.86 +/- 0.01	0.78 +/- 0.01	0.76 +/- 0.04	*0.80 +/- 0.03*
Distance traveled (m)	2.38 +/- 0.01	2.35 +/- 0.01	2.37 +/- 0.01	*2.37 +/- 0.01*
Elevation change (m)	1.33 +/- 0.01	1.35 +/- 0.01	1.28 +/- 0.01	*1.32 +/- 0.02*
Speed (m s^{-1})	2.78 +/- 0.02	2.96 +/- 0.02	2.63 +/- 0.02	*2.79 +/- 0.10*
Turn-rate (deg s^{-1})	127.5 +/- 2.8	135.7 +/- 3.1	127.1 +/- 2.8	*130.1 +/- 2.8*
Climb-rate (m s^{-1})	1.55 +/- 0.02	1.71 +/- 0.02	1.43 +/- 0.02	*1.56 +/- 0.08*
Wingbeat rate (Hz)	11.69 +/- 0.04	10.94 +/- 0.04	11.06 +/- 0.05	*11.23 +/- 0.23*

Flight behavior

On average it took the bats 0.80 +/- 0.03 seconds to pass through the corridor between the two nets (Table 3.1). In this amount of time, the bats traveled an average of 2.37 +/- 0.01 meters, climbed 1.32 +/- 0.02 meters, and flew at an average speed of 2.79 +/- 0.10 meters per second (Table 3.1). The bats reached maximum speed of 4.15 +/- 0.13 meters per second before the first net crossing, then decreased flight speed while in the corridor until reaching their minimum flight speed of 1.86 +/- 0.06 meters per second at the exit of the corridor (Fig. 3.2A). Once past the second net opening the bats increased speed to an average of 2.19 +/- 0.03 meters per second.

The two net openings and tethered insect were spaced along the width of the flight room, which required the bats to make multiple turns (Fig. 3.1C). The average turn-rate in between the nets was 130.1 +/- 2.8 degrees per second (Table 3.1), but turn rate was not constant. We calculated the instantaneous turn rate, aligned to each net crossing, and averaged across trials (Fig. 3.2B). The bats approached the first net at a low turn rate of 70.2 +/- 10.5 degrees per second. After crossing the first net opening, turn rates

increased to 143.4 +/- 15.0 degrees per second, then rapidly decreased to 44.82 +/- 1.7 degrees per second in between the nets. Then, as the bats approached the second net opening, turn rate increased to a maximum of 233.4 +/- 26.2 degrees per second. Turn rates remained high, with an average value of 122.9 +/- 14.4 degrees per second, after exiting the corridor.

The entrance and exit openings in the net corridor were offset in height, which required the bats to climb in elevation (Fig. 3.1D). The bats changed flight elevation by an average of 1.32 +/- 0.02 meters between the nets, which resulted in an average climb rate between the nets of 1.56 +/- 0.08 meters per second (Table 3.1). As the bats approached the first net opening, climb rate was, at first, negative (diving), but increased to a positive value before crossing the opening (Fig. 3.2C). The maximum climb rate of 1.78 +/- 0.05 meters per second occurred in the corridor between the two nets. As the bats approached the second net opening, climb rate decreased to 0.82 +/- 0.17 meters per second. After crossing the second net, climb rate further decreased to an average of 0.34 +/- 0.08 meters per second.

The average wingbeat rate of bats flying between the nets was 11.23 +/- 0.23 Hz (Table 3.1). Their wingbeat rate varied while navigating the nets (Fig. 3.2D). On the approach to the corridor, during the drop in elevation, the wingbeat rate was lower at 9.83 +/- 0.55 Hz. As the bat neared the first net opening, wingbeat rate increased to 12.76 +/- 0.40 Hz. After entering the corridor, the wingbeat rate decreased to 10.56 +/- 0.24 Hz. After exiting the corridor, wingbeat rate increased to 12.11 +/- 0.24 Hz.

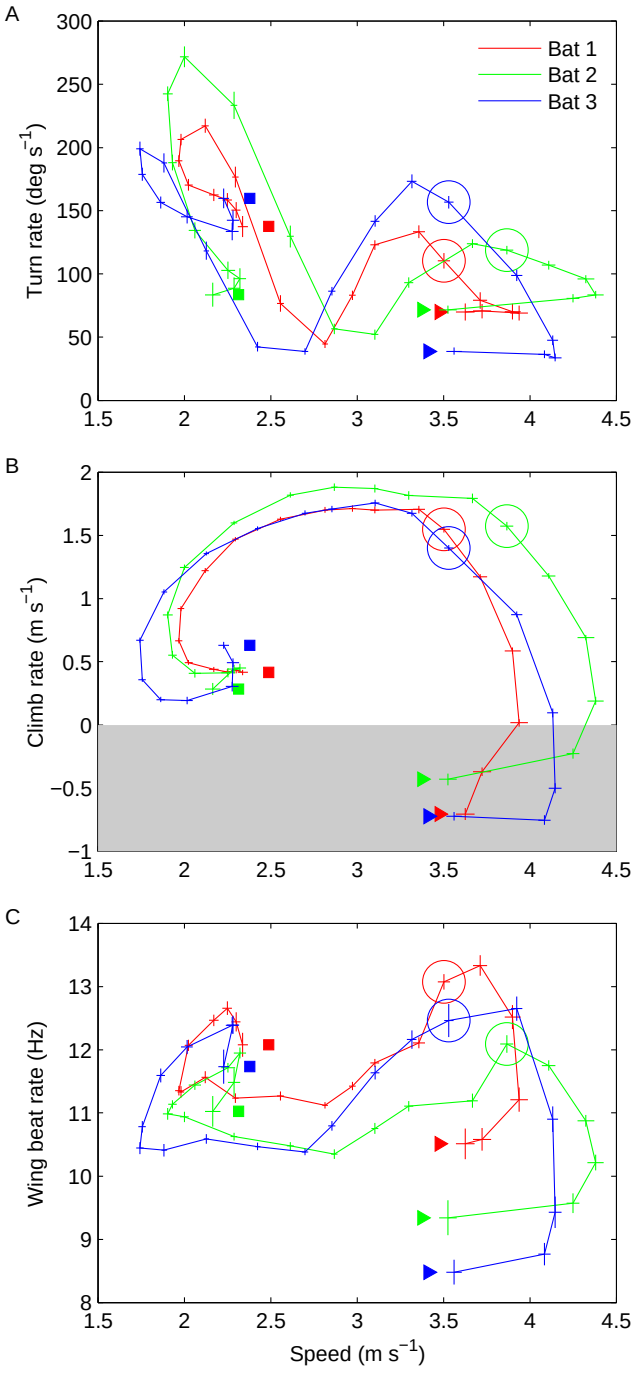

Fig. 3.3: Binned speed vs. climb rate (A), speed vs. turn rate (B), and speed vs. wingbeat frequency (C) for each bat. Bat 1 in red, 2 in green, 3 in blue. Data are aligned to the first net crossing and binned across 0.1 second intervals. Data are means +/- s.e.m (represented as the line length in each direction). Trial start (-0.5 seconds before first net crossing) indicated with right facing arrow, trial end (1.5 seconds after first net

crossing) indicated with square for each bat. The open circle indicates the last binned data before the first net crossing. Shaded region indicates negative climb rate (diving).

Flight speed, turn rate, climb rate, and wingbeat frequency changed as the bats navigated the net openings (Fig. 3.2). Flight speed influences the generation of lift (Pennycuick, 1968), and thus, could be used to predict the ability of the bat to make maneuvers with high turn or climb rates. However, in this experiment, we did not find flight speed to strongly correlate with climb, turn, or wingbeat rate (Fig. 3.3). We found that high turn rates more often occurred at low flight speeds, and that low wingbeat rates more often occurred at high flight speeds, but these results were likely influenced by the specific maneuvers required in relation to the nets. For example, each of the bats dove towards the first net opening, which produced high initial flight speeds before the climb and produced momentum for the bats to carry into the climb and the turn. The short trial time of less than 2.5 seconds and the specific maneuvers required in relation to the location of the nets did not allow for varied flight behavior and may have resulted in reduced correlation between flight speed and other flight parameters. However, the maneuvering required in the present study parallels natural flight maneuvers during insect capture and suggests an adaptable linking between flight speed and other flight kinematics.

Wingbeat frequency, amplitude, and Strouhal number

In this study, we found changes in wingbeat frequency over time, from 9-13 Hz, as the bats navigated the nets and captured the tethered insect (Fig. 3.2D), but no strong relationship between wingbeat frequency and flight speed (Fig. 3.3C). During the climbing portion of the trial, we examined the effect of the changing flight parameters on

force production and vortex flow. Wingbeat frequency (f), forward flight speed (U), and wing amplitude (A) determine the Strouhal number,

$$St = \frac{fA}{U} \tag{3.2}$$

a dimensionless number which describes oscillating flow mechanisms and predicts unsteadiness of the flow (G. S. Triantafyllou, Triantafyllou, & Grosenbaugh, 1993; M. S. Triantafyllou, Triantafyllou, & Gopalkrishnan, 1991). Bats, birds, and insects as well as non-fliers such as bony fish, sharks, and dolphins, tune their locomotion to a narrow range of Strouhal numbers, between 0.2 and 0.4, which is associated with efficient lift and thrust production in cruising flight (Taylor, Nudds, & Thomas, 2003). However, non-cruising, maneuvering, or slow speed flight occurs outside the range of favorable force production and Strouhal numbers, where unsteady flow may play a larger role (Norberg & Winter, 2006).

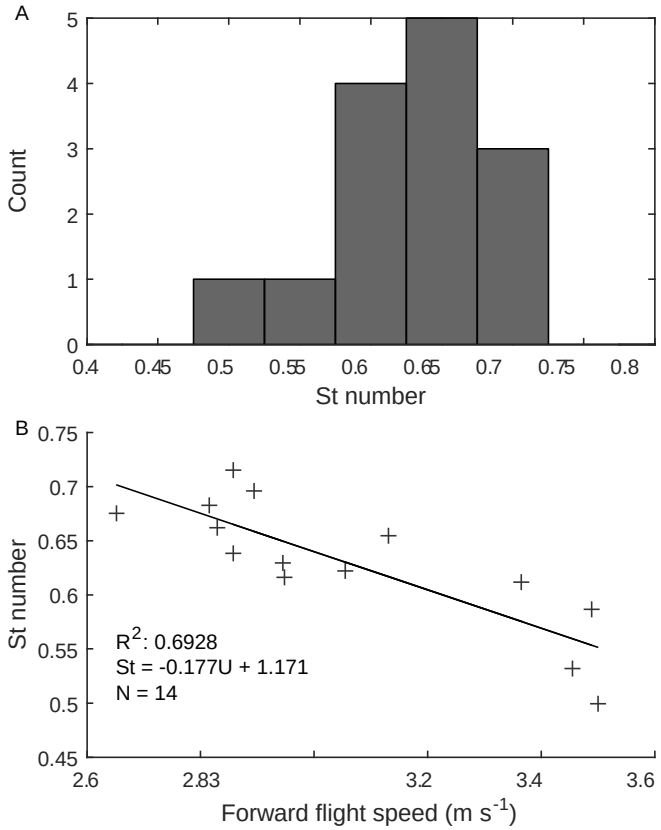

Fig. 3.4: (A) Histogram of measured Strouhal numbers. (B) Forward flight speed by Strouhal number. All wingbeat cycles in this analysis occurred during the climbing portion of the trial in between the two net openings.

We measured wing tip amplitude from motion capture data along entire wingbeat cycles during the climbing portion of the trial. Because of gaps in motion capture data with wing tip markers, only limited data were available (a total of 14 complete wingbeat cycles, wing tip marker data from the left wing tip, with bats 1 and 2). Using these data we calculated the Strouhal number after correcting for the climbing angle and found that Strouhal numbers fell outside the favorable range for force production (Fig. 3.4A). Our finding that Strouhal numbers fell in an unfavorable range indicates that the bats in this study likely experienced unsteady flow.

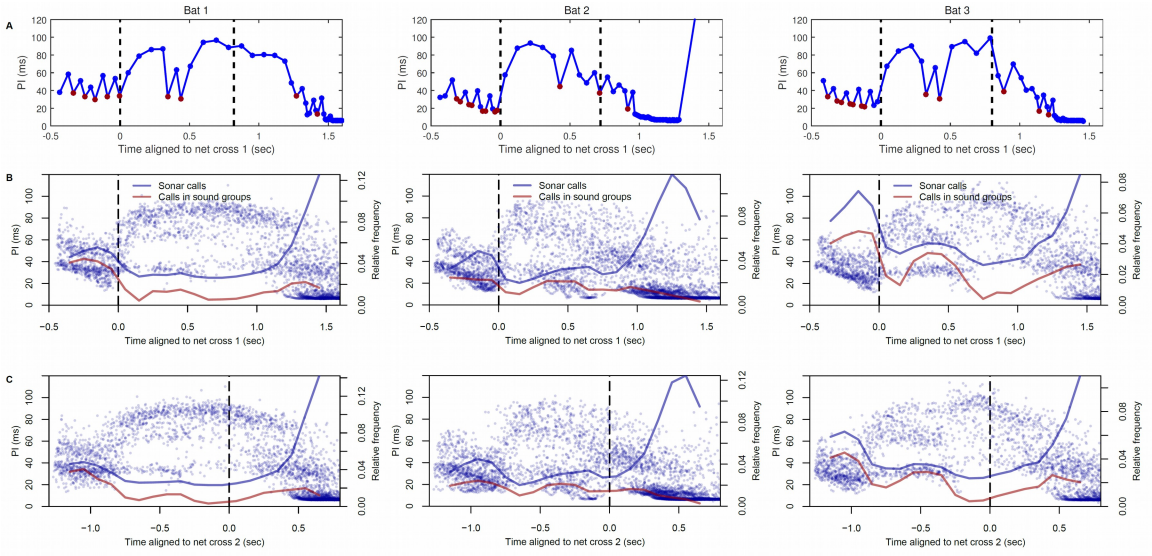

Fig. 3.5: Pulse interval (PI) relative to net crossings for each bat. Bat 1 in the left column, bat 2 in the middle column, and bat 3 in the right column. Top panels (A) show a single trial sequence for each bat. The PI for each sound group is highlighted in red, with all other vocalizations in blue. First and second net crossings indicated with dashed black lines. For the middle (B) and bottom (C) panels, the vocal data are aligned to the first net crossing and second net crossing. Each blue circle represents the PI of two calls in a trial sequence, and all trial sequences are plotted for each bat. The relative frequency of all sonar calls (blue) and sound group calls (red) is overlaid with line plots (bin size for relative frequency is 0.1 seconds). The vertical dashed black line signifies the aligned net crossing (time 0).

Sonar behavior

Sonar pulse interval (PI) is the time between sonar emissions, which is an indicator of echo information flow. We examined PI as the bats navigated the net openings and found that PI varied with the time to net crossing (Fig. 3.5). Single trials (Fig. 3.5A) revealed that the bats emitted sonar sound groups, or clusters of vocalizations with a stable PI surrounded by calls with a larger PI, in large numbers prior to the first net crossing. Single trials also showed sound groups between the nets, as well as before the terminal

buzz (see Movies 1, 2, and 3 in supplementary material). Across all vocal recordings (Fig. 3.5B, C), clusters of vocalizations with short PI and long PI are evident, which indicate sonar sound groups. We calculated the relative frequency, or the ratio of the call count from the total count, of all sonar emissions and sonar sound groups, and found that the relative frequency for sonar sound groups was highest prior to the first net crossing in all bats. After crossing the first net, sonar emissions, including sonar sound groups, decreased for a period of 0.2 seconds. The vocal emission rate then increased, as well as sound group emission rate, at 0.5 seconds before the second net crossing. Sound groups decreased in relative frequency as the bats approached the second net crossing, while overall emission rate remains stable. As the bats prepare to enter the terminal buzz, after crossing the second net opening, to catch the tethered insect, they often emitted sound groups. Bat 2 produced a buzz group before the second net opening in 8.70 % of trials, with an average pulse production rate in these trials reaching 155.07 +/- 1.83 calls per second.

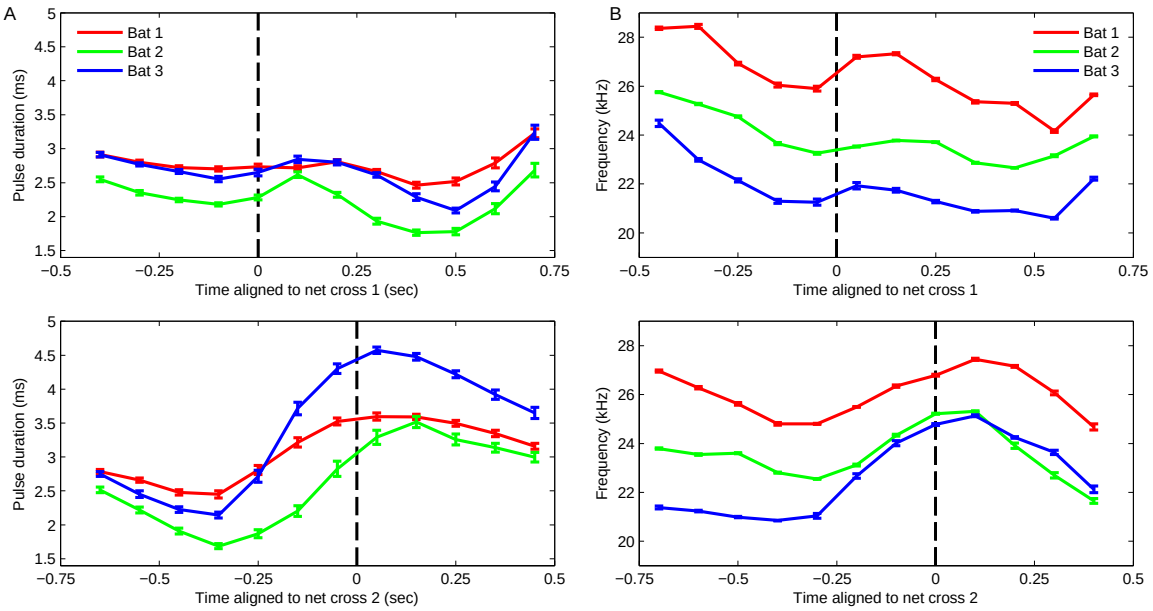

Fig. 3.6: Pulse duration (A) and pulse end frequency (B) relative to each net opening. Bat 1 in red, 2 in green, 3 in blue. Data was averaged across 0.1 second time bins, and error bars are s.e.m. Top panel: aligned to first net crossing; bottom panel: aligned to second net crossing. Only data with a PI greater than 10 ms were included in this analysis. Vertical dashed black line signifies net crossing (time 0).

The bats in this study altered the duration of their sonar sounds in relation to the distance to the net openings (Fig. 3.6A). The duration of sonar sounds analyzed ranged from less than 2 ms to more than 4.5 ms (terminal buzz calls were excluded from the analysis). The bats decreased pulse duration from 0.4-0.1 seconds before the first net crossing, from 2.79 +/- 0.12 to 2.48 +/- 0.16 ms. After crossing the first net opening, pulse duration increased to 2.73 +/- 0.07 ms. As the bats continued through the corridor, pulse duration decreased to 2.09 +/- 0.22 ms, at around 0.35 seconds before the second net crossing, as the bats prepared to exit the net corridor. However, as the bats approached the exit of the corridor, pulse duration increased, with a peak between 0.05 and 0.2 seconds after the

second net crossing at 3.86 +/- 0.31 ms. Pulse duration decreased to 2.84 +/- 0.16 as the bats continued and prepared to capture the tethered insect.

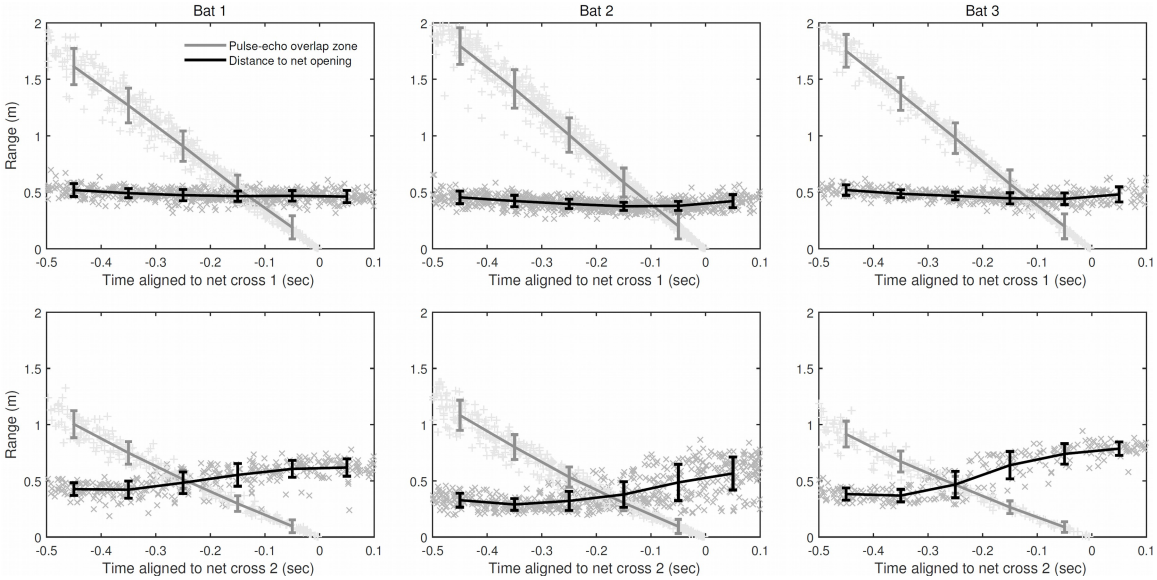

Fig. 3.7: Pulse-echo overlap zone relative to the distance to net opening across multiple trials. Pulse-echo overlap zone was the minimum distance an object could be to each bat without echoes from the net overlapping in time with produced pulses. Thick lines are means after aligning in time to each net crossing. Plotted are the pulse-echo overlap zone (black line) and the distance to net opening (gray line) with error bars as standard deviation. The values for each sonar call are plotted: calculated pulse-echo overlap zone (dark gray x symbols) and measured distance to net opening (light gray cross symbols). The top panels are crossing the first net opening and the bottom panels are crossing the second net opening. Left panels are bat 1, middle panels are bat 2, and the right panels are bat 3.

The pulse-echo overlap zone is the range in distance in which sonar emissions overlap with echo returns, which we calculated relative to the distance to each net opening prior to net crossing (Fig. 3.7). When approaching the first net opening, bats did not reduce pulse duration with decreasing distance to the net. As a result, the bats experienced

pulse-echo overlap with echoes from the net starting 0.11 +/- 0.01 seconds and 0.43 +/- 0.03 meters prior to net crossing. As the bats approached the second net opening, pulse-echo overlap occurred earlier, starting 0.22 +/- 0.02 seconds before net crossing, but at approximately the same distance, at 0.44 +/- 0.04 meters prior to net crossing. Bats 1 and 3 experienced pulse-echo overlap earlier than bat 2 as they approached the second net opening. Bat 2 experienced overlap later, at 0.18 seconds and 0.37 meters prior to net crossing. The bats' vocal and flight behavior resulted in pulses overlapping with the returning echoes from both of the nets.

We measured the end frequency of each sonar vocalization, excluding calls in the terminal buzz, to determine how the bats adapted the frequency content of their sonar signals with the net obstacles (Fig. 3.6B). There was a significant variation in call end frequencies between the individual bats, with a maximum difference of 5.5 kHz, but the bats changed end frequency as they navigated the nets in a similar pattern to each other, decreasing near the first net opening, decreasing between the nets, and increasing during the approach to the second net opening. The bats had an average end frequency at 0.4 seconds prior to the first net crossing of 26.2 +/- 1.2 kHz, and as they approached the first net opening, they decreased end frequency to 23.4 +/- 1.3 kHz. After crossing the first net opening, call end frequency increased, briefly, to 24.3 +/- 1.6 kHz, then gradually decreased or remained constant between the nets. The call end frequency as the bats approached the second net opening, at 0.7 seconds before net crossing, was 24.0 +/- 1.6 kHz. The bats decreased end frequency until 0.3 seconds before net crossing to an average of 22.8 +/- 1.1 kHz. The bats then increased end frequency as they approached

the second net crossing, to 25.2 +/- 0.7 kHz. After crossing the second net opening, end frequency increased slightly until 0.1 seconds after net crossing, after which end frequencies decreased sharply to 22.1 +/- 1.0 kHz at 0.4 seconds after net crossing as the bats prepared to capture the insect. End frequencies of calls in sound groups were not different from single calls produced outside of sound groups, and we also did not observe differences in end frequencies between calls within sound groups.

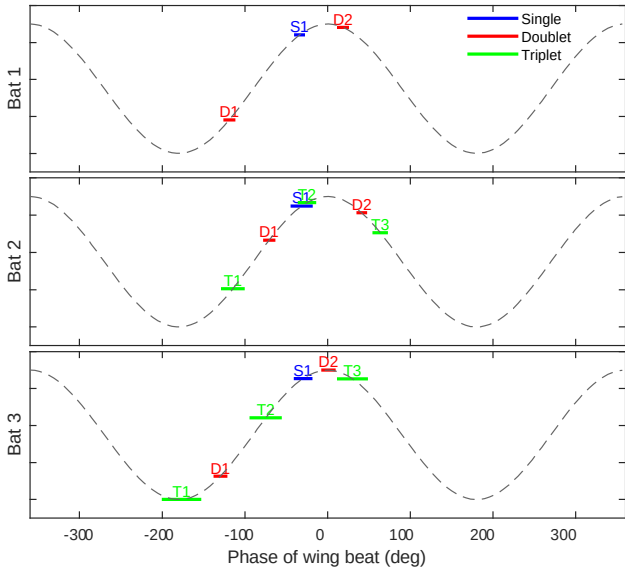

Fig. 3.8: Timing of sonar calls with respect to the phase of the wingbeat for each bat. Top panel: bat 1; middle panel: bat 2; bottom panel: bat 3. Plotted separately are single calls (blue), sonar sound groups of two calls (red), and sonar sound groups of 3 calls (green). The width of the lines are 95% confidence intervals. The order of each call within a sound group is indicated with a number above each value. Triplets that did not meet requirements for a 95% confidence interval were not plotted (this occurred only in bat 1). All non-buzz vocalizations were included from 0.5 seconds before the first net crossing to .075 seconds after the second net crossing for each trial.

Timing of sonar calls with wingbeat cycle

We calculated the relative timing of each sonar call with respect to the phase of the wingbeat for each bat (Fig. 3.8). We found that the timing of single echolocation signals (calls not part of a sound group) occurred close to and before the end of the upstroke for each bat, at -31.6 +/- 1.3 degrees in the wingbeat cycle. In sound groups with two calls (doublets), the first call occurred earlier at -106.4 +/- 18.2 degrees, while the second call in the doublet occurred later at 20.4 +/- 11.7 degrees. In sound groups with three calls (triplets), the first call occurred earlier at -144.1 +/- 18.0 degrees, close to the beginning of the upstroke. The middle call in the triplet occurred at -55.4 +/- 15.4 degrees. The third call in the triplet occurred during the downstroke at 40.1 +/- 11.8 degrees. There was variation in the specific timing of doublets and triplets between bats, but single calls had the least variation and occurred near the apex of the wingbeat cycle in all bats.

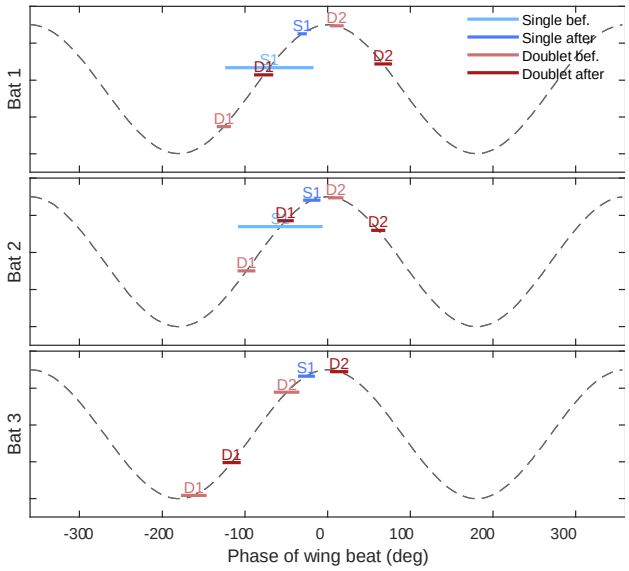

Fig. 3.9: Timing of sonar calls with respect to the phase of the wingbeat before and after the first net crossing for each bat. Plotted separately are single calls (blue) and doublet sonar sound groups (red). Calls before the net crossing have light shading and calls after the net crossing have dark shading. The width of the lines are 95% confidence intervals. The order of each call within a sound group is indicated with a number above each value. Single calls prior to the first net opening for bat 3 did not meet the requirements for confidence intervals and was not plotted. Triplets did not meet requirements for 95% confidence intervals along this time scale and were excluded from the analysis. The period of time for inclusion was 0.5 seconds on either side of the first net crossing.

We examined the timing of calls relative to wingbeat phase either before or after the first net crossing for each bat (Fig. 3.9). Single calls were not emitted in large numbers before the first net opening, which restricted our ability to characterize and compare the relative wingbeat phase for these calls. However, we did notice a trend in bats 1 and 2, with single calls occurring later in the wingbeat phase after the bat crossed the net opening. Sonar calls in sound group doublets were also shifted to a later wingbeat phase after the net crossing, with the first call in doublets shifted from -128.6 +/- 18.4 to -81.4 +/- 18.9

degrees and the second call in doublets shifted from -9.6 +/- 20.0 to 47.3 +/- 16.8 degrees.

Discussion

This study investigated the coordination of flight and echolocation behaviors in the big brown bat, *Eptesicus fuscus*, as it negotiated a flight corridor to gain access to a tethered prey item. Bats made adjustments in flight speed, turn rate, and climb rate, which coincided with adaptive changes in sonar behavior. In addition, bats adjusted the timing, duration, and frequency of sonar vocalizations in relation to obstacle navigation and insect capture. In straight flight, bats produced sonar calls in phase with the upstroke of the wingbeat cycle, but that relationship changed when the bats navigated through openings in the net corridor.

Strouhal number

A study by Norberg and Winter (2006) showed that the hovering nectar feeding bat, *Glossophaga soricina*, achieved efficient Strouhal values at high flight speeds, but at low flight speeds, the Strouhal number increased to values which incur unsteady effects. We found that flight speed was a predictor of Strouhal number in this experiment (Fig. 3.4B), which confirmed in the big brown bat that slow forward flight speed occurs with high Strouhal numbers and unsteady flow. It is noteworthy that wingbeat frequency of *E. fuscus* did not correlate with Strouhal number.

At low speeds, hovering bat species produce a backwards flip of the wing tip (Norberg, 1970; Norberg & Winter, 2006), which has been suggested to generate lift (Norberg, 1976b). Hovering bats have also been found to take advantage of a leading edge vortex to generate lift when flying at slow flight speeds (Muijres et al., 2008, 2014). In the present study, *E. fuscus* was never observed making a backwards flip of the wing tip, so this source of potential lift would not be available. While *E. fuscus* primarily forages in open space, it also hunts in cluttered environments, in and around vegetation, where it flies at slower speeds (Falk, Jakobsen, Surlykke, & Moss, 2014; J. A. Simmons et al., 2001). Thus, unsteady flow effects, and alternate forms of generating lift, may occur when *E. fuscus* flies at slow speeds.

Adaptive sonar behavior

The bats in the present study adjusted sonar behavior with respect to the net openings by altering the rate of overall call production, with an increase in sonar sound groups, call duration, and call end frequency (Fig. 3.5, Fig. 3.6). Producing calls with shorter PI, when bats flew near the nets, increased the rate of echo returns and may have helped the bats localize the net openings. The PI of calls produced by bats approaching the second net opening were not as short as those produced by bats approaching the first net opening. The second net opening was larger than the first net opening (area 0.51 m^2, compared to 0.27 m^2), which may have decreased localization requirements and reduced the need for high pulse production rate.

The bat encountered two net crossings in this task, each requiring different aerodynamic maneuvers. The first net crossing occurred after a dive, as the bat entered the corridor from the open room, while the second net crossing occurred after a steep climb at slow flight speeds and high turn rates. Thus, it is not surprising that the echolocation behavior of the bats was different under these two conditions. For example, the flight speeds of the bats approaching the first net opening were approximately twice those of bats approaching the second net opening, which likely decreased rapid localization requirements during the second net crossing. Once inside the net corridor, the bats could have relied more heavily on spatial memory than echo information for navigation, and, combined with their slower approach, which would have allowed more time for planning the second net crossing. Furthermore, the lower call rate of bats during the climb and turn within the corridor can be understood in terms of combined energetic costs of the flight and vocal motor behaviors.

Sonar sound groups

Bat echolocation sound groups, clusters of calls flanked by signals with longer intervals, are produced when animals encounter challenging sonar tasks requiring figure-ground segregation and accurate measurement of target position (Kothari et al., 2014; Moss et al., 2006). These sound groups are therefore hypothesized to support high resolution sonar information (Moss & Surlykke, 2010). In this study, bats emitted sonar sound groups at relatively high rates prior to navigating the first net opening and again between the nets, as they prepared to exit the second net opening (Fig. 3.5). The shorter pulse

intervals of sonar sound groups could allow the bat to sample spatial information with greater reliability (Moss et al., 2006), which would aid in navigation around obstacles.

Emitting sounds in phase with the expiration cycle of respiration can be energetically advantageous (Speakman, Anderson, & Racey, 1989; Speakman & Racey, 1991), so even as the bats increased call production rate, they timed their call emissions, both within sound groups and single calls produced outside of sound groups, with the rising phase of the wingbeat cycle (Fig. 3.8). Koblitz et al. (2010) reported very similar patterning of calls with respect to the phase of the wingbeat cycle. These authors also found that source levels varied with the wingbeat phase. We propose that patterning of sonar calls into groups allows bats to increase echo information flow without incurring large energy costs (Speakman & Racey, 1991).

Duration adjustments and inner window with respect to net position

As species of bats emitting FM sonar signals approach a target, they typically reduce the duration of their sonar sounds to avoid temporal overlap between their emitted pulses and returning echoes until the final phase of the terminal buzz (Kalko & Schnitzler, 1989; Schnitzler & Kalko, 2001). We found that as the bats navigated each net opening, they failed to reduce call duration to avoid overlap between their emitted sonar sounds and the returning echoes from the nets (Fig. 3.7). In fact, the bats increased pulse duration when approaching the second net opening, which resulted in an overlap between pulse and net echo as early as 250 ms before the net crossing.

The increase in call duration prior to the second net crossing, may reveal a shift in acoustic gaze to the insect behind the net. Longer duration calls are better suited for detection, as they return higher energy echoes. Two previous studies found that bats navigating a single net opening, prior to capturing an insect, produced sound durations which overlapped with returning echoes from the net (Jensen et al., 2005; Surlykke et al., 2009). Surlykke et al. (2009) measured the aim of the sonar beam and reported that the bats directed their sonar beam on the more distant insect before they crossed the net opening while they experienced pulse-net echo overlap. Thus, as in the report by Surlykke et al. (2009), the bat's failure to decrease call duration to avoid pulse-net echo overlap in this study, may serve as an indicator that the animal shifted its attention to the more distant prey item beyond the second net crossing. We infer that during this segment of the trial, the bats may have relied on spatial memory for navigation.

End frequency changes suggest changes in directionality

Jakobsen & Surlykke (2010) found that bats achieve a broadening of the sonar beam, and a widening field of view, by decreasing the frequency content of their sonar calls during terminal buzz, while keeping the effective sonar emitter size constant. In the present study, we found fine scale changes in sonar call end frequency which occurred as the bats maneuvered in flight around obstacles (Fig. 3.6B). If we assume a constant emitter size, 5.9 mm as reported by Jakobsen and Surlykke for *Eptesicus serotinus*, a similar bat species to *E. fuscus*, we can estimate the beam width using a simple piston model (Strother & Mogus, 1970). As the bats approached the first net opening, they decreased end frequency of the FM sweep from 26.2 to 23.4 kHz, which, according to the model,

would increase the half amplitude angle of their sonar beam by 10 degrees, from 51 to 61 degrees. When approaching the second net opening to just after the second net crossing, the bats increased end frequency from 22.8 to 25.9 kHz, which would decrease half amplitude angle by 12 degrees, from 64 to 52 degrees. These results indicate that bats manipulate their sonar beam width as they maneuver around obstacles and suggest fine scale control of the sonar beam to adjust sonar field of view and search volume.

Timing of sonar calls in relation to wingbeat phase and net position

As discussed by (Koblitz et al., 2010), the coordination of sound groups with the wingbeat cycle indicates that call timing is planned several tens or hundreds of milliseconds in advance of production. The present study confirms that sound groups occur at consistent phases of the wingbeat cycle (Fig. 3.8). However, we also found that the relative timing of calls in relation to the wingbeat cycle changed when bats negotiated the turn and climb around the first net opening (Fig. 3.9). These differences in vocal patterning could be related to wingbeat irregularities during maneuvering. The shift in call timing pattern with respect to the wingbeat cycle likely resulted in changes in echo intensity, which we could not measure directly in this study. Timing of sonar calls relative to the wingbeat cycle appears to be adaptable and possibly influenced by task requirements and corresponding flight kinematics.

Conclusion

As a bat navigates and forages in cluttered environments, it must make precise and rapid adjustments in flight kinematics and echolocation call features. By quantifying the motor behaviors of bats engaged in a navigation task, we discovered that flight kinematics and echolocation call features were not only dependent on the spatial relation between the bat and obstacles, but tightly coordinated to execute integrated motor planning of sonar-guided orientation.

Acknowledgments

We would like to thank Delphia Varadarajan for assistance with data collection and Enamul Haque for assistance with data analysis. We also thank Susanne Sterbing-D'Angelo for comments on the manuscript.

Chapter 4: Bat flight kinematics in wind gusts

Abstract

We report flight trajectory and wing kinematic data from a behavioral study in which bats encountered wind gusts as they performed an obstacle avoidance and prey-capture task. Wind gusts were introduced randomly from different directions as the bats maneuvered through a narrow opening in a net to gain access to a tethered insect one meter beyond the opening. The effects of air turbulence on flight maneuverability were quantified with high-speed video and motion-capture recordings. Bats were able to successfully fly through the gust of wind to reach the food reward. We characterized adaptations in flight speed, turn rate, climb rate, wingbeat rate, and relative position to the net opening in relation to the obstacle navigation and wind gust treatment. Bats adapted flight kinematics to reach the insect target by adjusting bank angle and Strouhal value, an index of the steadiness of the flow. The results of this study reveal that bats make rapid adaptive changes in flight kinematics to successfully maneuver under wind gust conditions.

Introduction

Bats engage in highly maneuverable flight as they navigate around obstacles and hunt for evasive prey. In the natural environment, bats also face the challenge of diverse weather conditions, including sudden gusts of wind. There are conflicting reports as to whether bats reduce activity on nights with high wind speeds (Johnson, Gates, & Zegre, 2010), or whether wind speed and bat concentrations are positively correlated (Russ, Briffa, &

Montgomery, 2003). Bats have been observed flying in wind speeds of more than 4.5 meters per second (O'Farrell & Bradley, 1970), and have also been found to forage in high wind speeds along the leeward side of trees where insect concentrations were high (Racey & Swift, 1985). If bats reduce activity during windy nights, it may not be due to their own flight capabilities but instead a reduced availability of insect prey. Even if bats avoid flying in steady winds, they must still function in unpredictable wind gusts, which can cause turbulent airflow on the wings and a disruption of laminar flow and stall. To the best of our knowledge, there are no studies of bat flight in wind gusts.

Bats adjust wing kinematics to generate aerodynamic forces to meet different flight requirements, varying wingbeat frequency and wingbeat amplitude, the path of the wing relative to the body, the angle that the wing meets the air, as well as the wing curvature and wing surface area (Hedenström & Johansson, 2015; Swartz, Iriarte-Díaz, Riskin, & Breuer, 2012). Bat wings contain a compliant wing membrane connected to the body with flexible wing bones (Swartz, 1997). Bats also have muscles in the wings, which may control mechanical properties of the wing membrane (Norberg, 1972). Collectively, the adjustments in bat flight kinematics allow for rapid changes in flight speed, turning, and climbing.

Steady-state aerodynamic theories do not fully explain the lift forces needed to sustain bat flight, especially in slow and hovering flight (Hedenström et al., 2007). The airflow across bat wings can be complex, with a different vortex structure than that of bird flight. One unsteady mechanism for generating lift is the leading edge vortex (Muijres et al.,

2008), which has been found during slow flight but not fast flight (Muijres et al., 2014). A recently proposed model of flapping counter-torque has demonstrated that during slow and hovering flight, symmetric wing flapping can be used to control turning (Hedrick, Cheng, & Deng, 2009). However, the details of how bats fly during slow and maneuvering flight are not yet fully understood.

Kinematic studies of bat aerial locomotion have mainly focused on flight inside wind tunnels (Hubel et al., 2012; Schnitzler, 1971; Von Busse, Hedenström, Winter, & Johansson, 2012; Wolf, Johansson, Von Busse, Winter, & Hedenström, 2010) or inside small volume flight cages (Norberg, 1970, 1976a, 1976b), where detailed measurements can be made more easily while controlling for flight and air speed. There have been some studies of maneuvering and turning flight in bats (Aldridge, 1987; Rayner & Aldridge, 1985), and one known study that includes detailed measures of flight kinematics (Iriarte-Díaz & Swartz, 2008). Further studies of bat flight during maneuvering, turning, climbing and foraging in larger spaces and under variable wind conditions are needed to better understand natural flight behaviors.

In the present study, we examine how the big brown bat, *Eptesicus fuscus*, navigates an obstacle to capture a tethered insect. On select trials, we delivered a wind gust from one of three different directions and monitored flight trajectories and wing kinematics to discover changes in flight performance, trajectories and kinematics as the bat encountered wind gusts.

Methods and methods

Four adult, wild-caught big brown bats (*Eptesicus fuscus*) were trained to participate in these studies and complete data sets were collected from three of these animals. All experimental procedures were approved by the Institutional Animal Care and Use Committee at the University of Maryland, College Park.

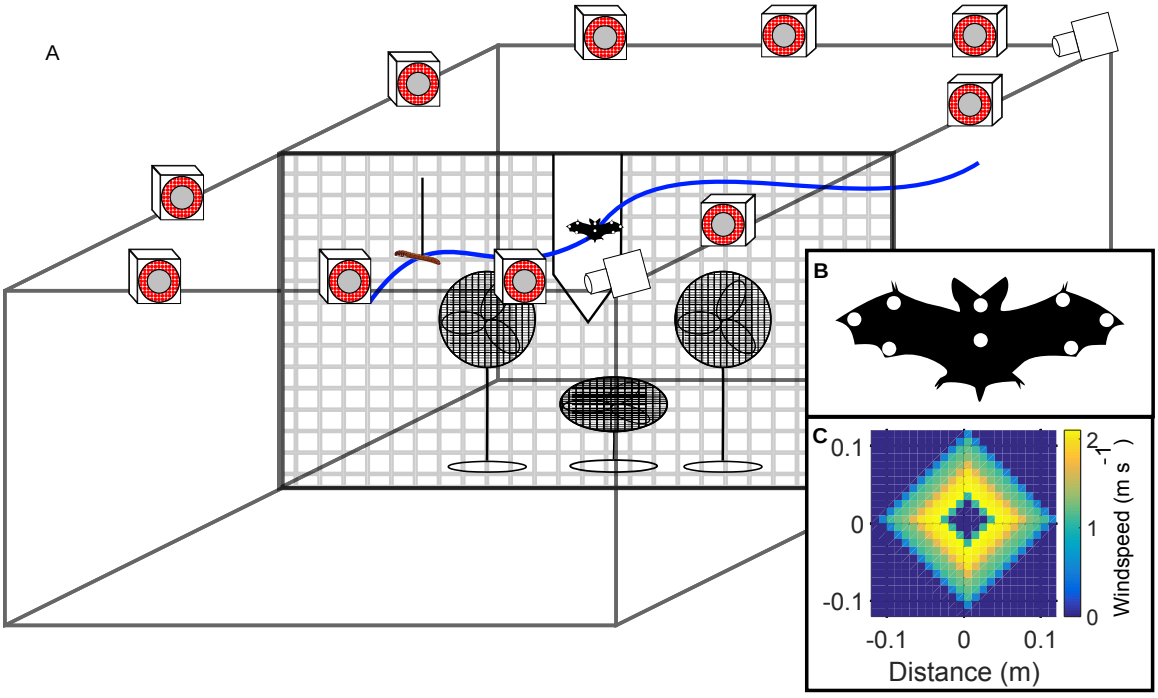

Fig. 4.1: Schematic of experimental setup (A), reflective marker placement on the bat (B), and wind speeds measured from the fan (C). (A) Motion-capture cameras shown with infrared lighting ring around lens (red circles) tracked the 3D position of reflective markers placed on the bat. High speed video cameras in two corners of flight room. Flight trajectory in blue, tethered insect in brown, and bat and floor-mounted fans depicted in diagram. (B) Marker locations shown as white circles on diagram of bat. (C) Wind speeds (m s^{-1}) measured at 0.5 m in front of the fan.

Experimental setup

All recordings took place in a laboratory flight room (7.3m x 6.4m x 2.5m) lined with sound absorbing foam (Sonex One, Acoustical Solutions, Inc.) under low light conditions at the University of Maryland, College Park (Fig. 4.1A). A net constructed of deer block netting (PVC mesh, 1.5 cm x 1.5 cm holes) spanned the width of the flight room and was suspended from the ceiling and attached to each wall with paper clips. The bats were trained to fly through an opening in the net near the center of the room (width 0.48 m, height 0.99 m, area 0.43 m^2) and capture an insect (*Tenebrio molitor* larvae) on the other side of the net, tethered and hanging from the ceiling by monofilament fishing line (Berkley Trilene, 0.9 kg test, 0.13 mm diameter). Three floor-mounted oscillating fans (side fans: Lasko 1820, lower fan: Honeywell) were placed at the entrance of the net opening and were switched on and off with a wireless remote. The side fans were placed 0.5 meters from the bottom and sides of the net opening and aimed upwards. The lower fan was aimed upwards and rested 0.2 meters from the ground. The wind speed from the side fans were measured using an anemometer (La Crosse Technology EA-3010U). Wind speed at 0.5 m from the fan was measured across the width of the fan (Fig. 4.1C). Maximum fan speed was 2.1 meters per second, a small area in the middle of the fan registered no wind speed, and no wind was measured outside of 0.12 meters from the center of the fan. The direction of wind for each trial was randomly selected, originating from one of the fans on either the left, right or below the net opening. In 30 % of the trials, the fans were not activated, and no-wind was introduced. The first two trials of each day always had no-wind, while the following trials had an equal probability of the four conditions (wind from left, right, below, or none).

Data recordings

For bats 1, 2 and 3, we collected 125 trials each across 5 consecutive days, of which we extracted trajectories from 116, and 119, and 116 trials. Of these, we excluded from detailed trajectory and kinematic analyses trials in which there were problems in the recordings, crashes into the net, or the bat did not attempt to capture the tethered insect after crossing the net opening, which resulted in 106, 112, and 108 trials remaining for bats 1, 2, and 3.

Motion-tracking recordings from 10 cameras at 370 frames per second (Vicon MX T40) allowed reconstruction of the bat's flight path and kinematic analysis of wing motion in 3D. High speed video recordings from two cameras (Photron FASTCAM PCI-R2 512) supplemented the motion-tracking recordings and were used to confirm motion-tracking data. The high speed cameras were synchronized and frame locked to one quarter the frame rate of the motion-capture cameras (93 frames per second). Motion-tracking was achieved using the Vicon Nexus software and data was exported to MATLAB (Mathworks) for further analysis. Reflective markers, 6.35 mm diameter, were attached to the wings of the bats and were cut out circles of reflective tape (3M 7610WS). On each wing, markers were placed at the thumb joint, the base of the wing near digit five, and at the wing tip on both the dorsal and ventral sides (Fig. 4.1B). Markers were fixed to the bat using tape adhesive and were replaced each day if any fell off. Hemispherical markers were also attached to the body and the head with eyelash glue (DUO white/clear). Data synchronization was achieved using a trigger switch that broadcast a

TTL signal to both systems. Each system was configured with an 8 second rolling buffer aligned to the onset of the TTL pulse.

Trajectory measurements

We calculated measures of flight speed, turn rate, climb rate, and wingbeat rate from a centroid of the motion tracked markers on the bats (smoothed using a 60 point moving average weighted by the number of reflections recorded within each frame). Gaps in the smoothed centroid, due to missing marker reflections, were interpolated using a spline function. Wingbeat oscillations were removed when calculating speed, turn rate, and climb rate using a low-pass Butterworth filter (cutoff frequency 6 Hz, order 6 with zero phase). The instantaneous speed of the bat was calculated as the distance traveled by the bat between each frame. The instantaneous turn rate was calculated as the difference in angular flight direction along the x/y plan projection between each frame, and smoothed using a 60 point moving average. The instantaneous climb rate was calculated as the difference in elevation between each frame.

For wingbeat calculations, the original unfiltered centroid data was filtered with a 15 point moving average, weighted by the number of reflections recorded within each frame. The altitude values in this smoothed centroid were band-passed (Butterworth filter, cutoff frequencies 6 and 20 Hz, order 12 with zero phase) in order to isolate wingbeat oscillations. We determined the locations of the wingbeat peaks and troughs using the findpeaks MATLAB function. An instantaneous phase of the wingbeat was calculated from the analytic signal (Hilbert transform of the smoothed and band-pass filtered altitude data).

Occupancy histograms were created using the smoothed flight trajectories and collapsing the data to a 2 dimensional plan projection (*x,y*). We counted the number of times the bat was present in 10 cm^2 sized bins, and normalized for the number of trials, creating probabilities of occupancy.

Motion-tracking labeling

Motion-tracking data was exported from Vicon Nexus to Matlab and processed using custom software, viconLabeler (Falk, 2015), to label the 3D points. Each 8 second recording was cropped to 3 seconds, 1.5 seconds on either side of the net crossing. All reflected points in this cropped recording were "rated" based on a 5 point track created from other points in consecutive frames joined together based on a nearest neighbor algorithm. Each rating was ordered based on the variation in speed and variation in angular direction, and the ratings with the lowest variation (top 10%) were chosen as tracks. Tracks were created from the initial 5 point rating and extended in each direction based on a nearest neighbor algorithm. Tracks ended when the speed or angular direction passed their respective thresholds (2 times the current speed of the track, a difference of 60 degrees in angular direction from the previous point). These tracks were then displayed in a GUI and manually labeled. We labeled a total of 45 trials from bat 1 including 24 trials from the no-wind condition and 21 from the wind condition (7, 9, 5 from below, left, and right wind directions respectively).

Kinematic measures

Bank angle measurements were calculated as the angle between the vector of the left and right wing markers and the floor. We used the thumb joint, digit 5, or wing tip markers. When more than one marker type was present, we calculated an average between the two angles. We were able to calculate the bank angle an average of 80 % of the frames in each trial.

We calculated the Strouhal number, a dimensionless parameter that describes oscillating flow mechanisms and can be a predictor of the unsteadiness of the flow. The Strouhal number is defined as:

$$St = \frac{fA}{U} \tag{4.1}$$

where f is the wingbeat frequency, A is the wingbeat amplitude, and U is the forward flight speed. For each wingbeat with marker data, we calculated the instantaneous wingbeat frequency, forward flight speed, and wingbeat amplitude, or excursion of the wing tip, after correcting for turn angle and climb angle. We gathered two measures for each wingbeat, one for the left wing tip marker and one for the right marker. When both left and right measures were present, we used a mean of the two measures.

Results

We collected data from three bats trained to fly through a net opening and capture a tethered insect. On each trial, a wind gust was applied from one of three different directions, bottom, left, or right, which the bats had to pass through in order to reach the

food reward (Fig. 4.1). In approximately 30 percent of the trials, there was no-wind gust introduced. The minimum distance across trials between the bat flight trajectory and any one of the fans was 0.43 +/- 0.10 m.

Performance

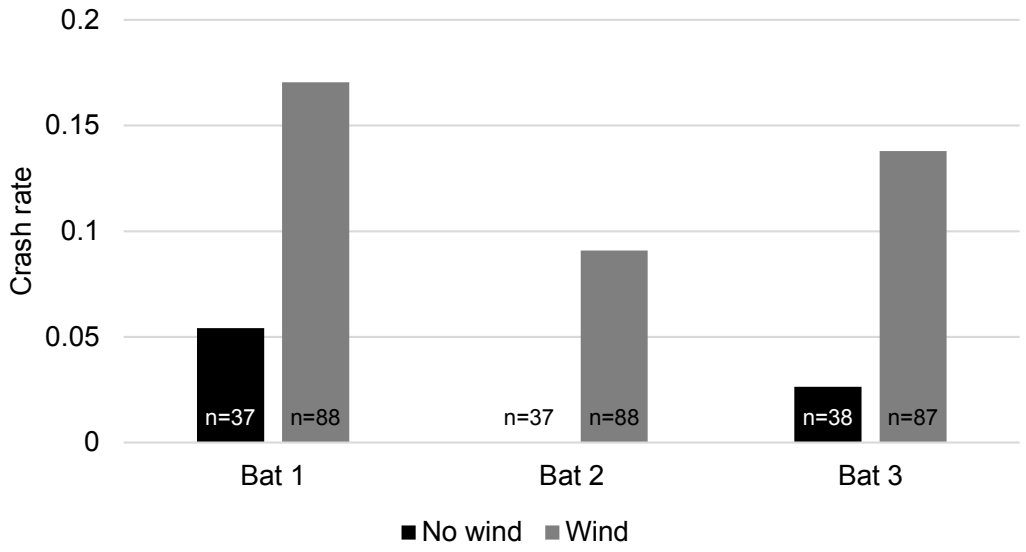

Fig. 4.2: Crash rate (percent of trials) into net compared between no-wind and wind conditions for each bat. The total number of trials in each condition for each bat is shown at the base of each bar.

In some trials, the bats crashed into the net as they attempted to pass through the net opening. We analyzed the rate of crashing for each bat for wind and no-wind condition trials (Fig. 4.2). A test of proportions did not yield a significant difference between conditions of wind and no-wind (Wilcoxon signed rank test, $p = 0.125$, $N=3$). However, we observed a consistent increase in the crash rate percentage for each bat during wind condition trials.

Trajectories

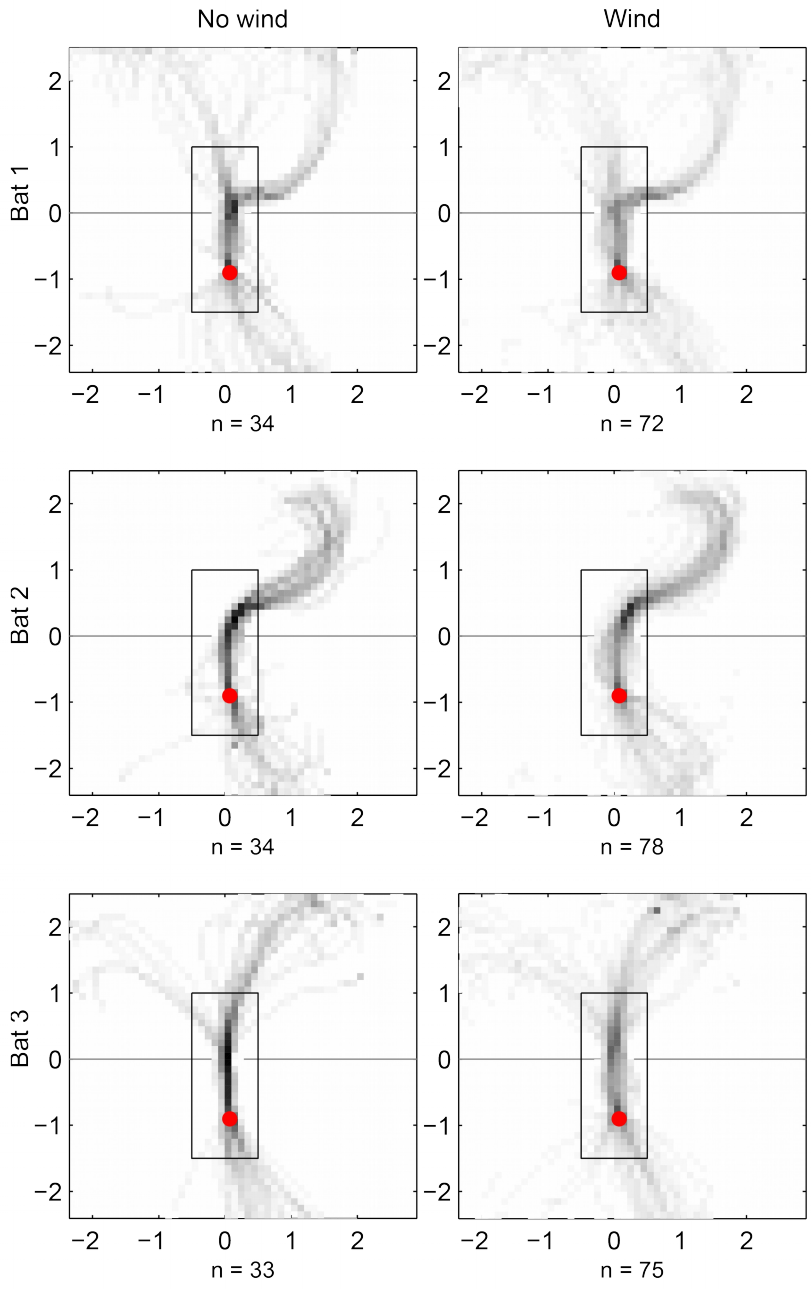

Fig. 4.3: Occupancy histograms of the 2D trajectories 0.75 seconds before and 0.75 seconds after net crossing for each bat. No-wind condition trials on left panels and wind condition trials on right panels. Tethered insect position is plotted as red circle, and the net as a gray line. The number of trials analyzed in each condition is at the bottom of each plot. Trials included for trajectory analysis required a direct flight through the net opening to the insect capture. The area of position data used for calculating the occupancy

histogram peak and spread is shown with the black rectangle around the net position.

Stereotyped flight paths can develop over time and indicate the bat's reliance on spatial memory (Barchi et al., 2013). We created occupancy histograms of trajectory data for each bat and compared between no-wind condition trials and wind condition trials (Fig. 4.3). Bat flight trajectories were stereotyped as they approached and navigated the net opening and captured the tethered insect. Bat 2 showed extremely stereotyped behavior during the no-wind condition as it approached the net opening from the same direction in each trial. As the bats encountered wind gusts, their trajectories were altered. We found that during wind condition trials, the trajectories became more variable, especially immediately before and after the net crossing, when the bats experienced the wind gust, recovered from the wind gust, and captured the tethered insect.

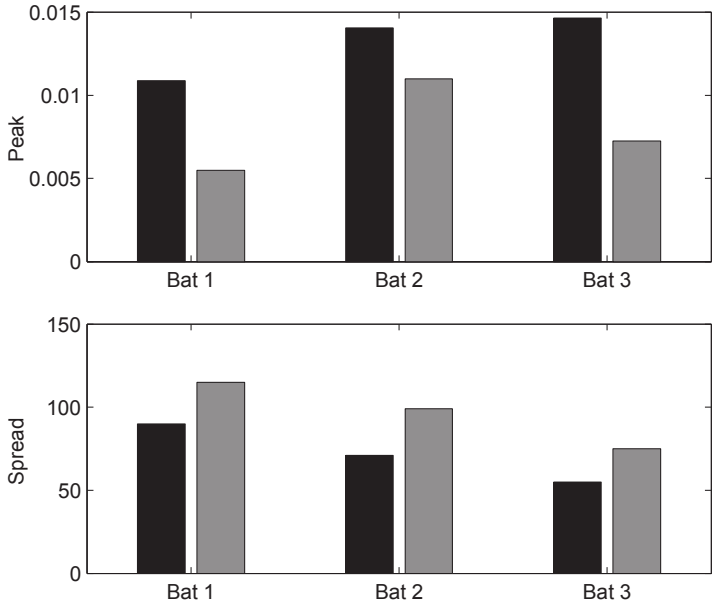

Fig. 4.4: Occupancy histogram values of peak (top panel) and spread (bottom panel) for no-wind condition (black) and wind condition (gray) for each bat. The peak was the maximum value of the occupancy histogram and the spread was the number of bins above the 60th percentile of the occupancy histogram within the rectangular area (see Fig. 4.3).

We compared the occupancy probability distributions between no-wind and wind conditions for each bat and found a difference between the no-wind condition and wind condition (Kolmogorov-Smirnov test, $p<.001$ for bats 1, 2, and 3). We also analyzed within the area of the occupancy histograms where the bats maneuvered through and recovered from the wind gust (rectangular area in Fig. 4.3). We calculated two measures from the occupancy histograms, the peak and the spread (Fig. 4.4). The peak occupancy value was calculated as the maximum occupancy value across bins for each condition and bat. The spread occupancy value was calculated as the number of bins above the 60th percentile for each condition and bat. We found that the peak occupancy value was larger in no-wind conditions, but not significantly different from the wind condition

(paired t-test, p=0.052, N=3). We found that the spread occupancy value was significantly lower during no-wind conditions than during wind conditions (paired t-test, p=0.009, N=3).

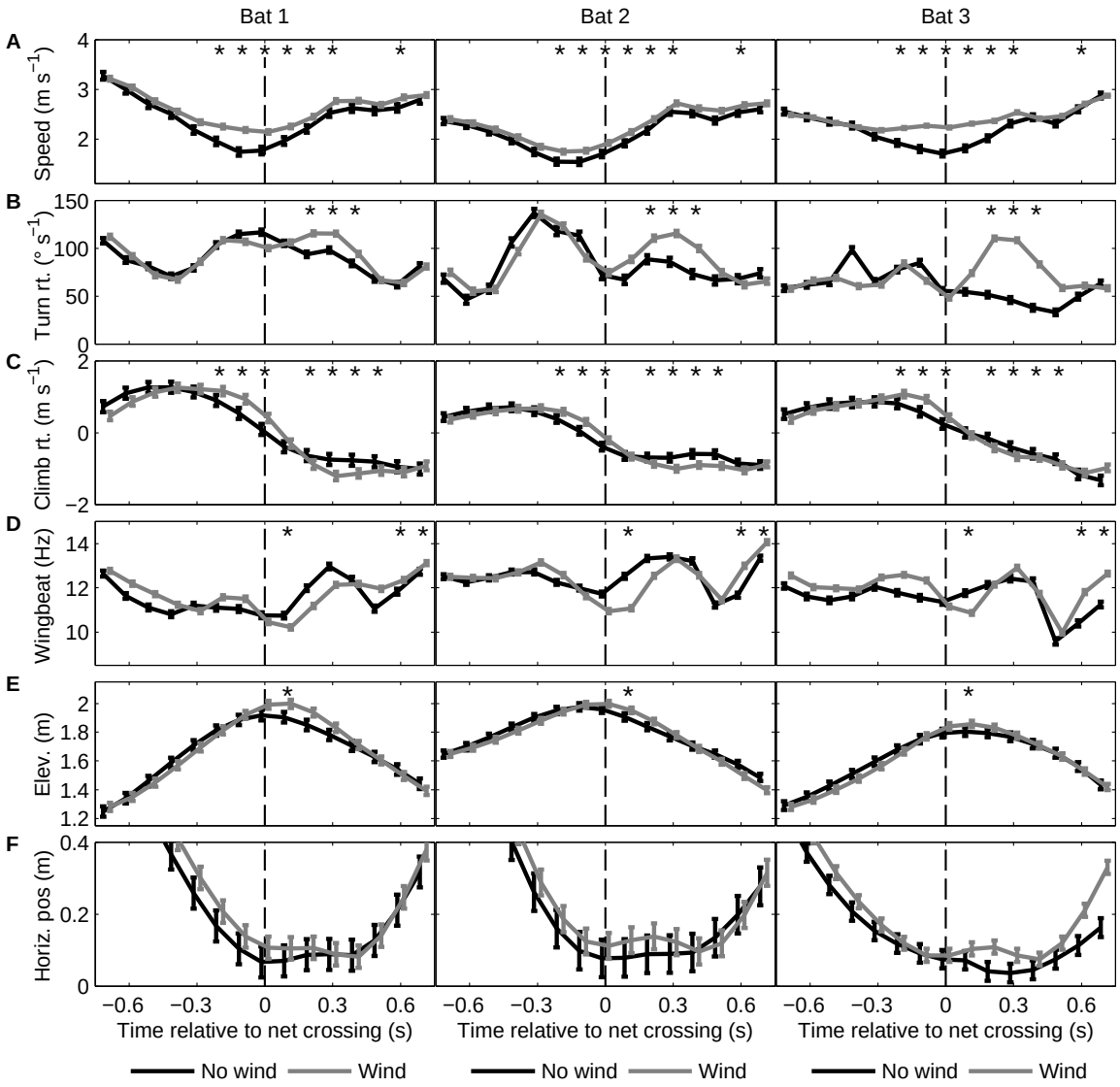

Fig. 4.5: Average trajectory measures by bat aligned to net crossing for no-wind (black) and wind conditions (gray). We measured flight speed (A), absolute value of turn rate (B), climb rate (C), wingbeat rate (D), elevation (E), and absolute value of horizontal position relative to the net center (F). Values are means +/- S.E.M. Statistically significant differences between no-wind and wind conditions indicated with the asterisk symbol above each bin. The time position of values are offset between the conditions to allow easier comparisons (+/- 0.015 s). The time of net crossing is indicated with a vertical dashed line. Wind was applied before the net crossing during wind condition trials.

We compared the flight trajectories across trials between no-wind and wind conditions using measures of speed, turn rate, wingbeat rate, elevation, and horizontal position (Fig. 4.5). Trajectory measures were calculated from the smoothed centroid of points reflected and recorded by the motion-tracking system (see Methods). Crash trials and trials in which the bats did not attempt to capture the tethered insect after crossing the net opening were not included in this analysis. For each measure, we compared the two-way interaction between wind condition and time relative to net crossing (two-factor, within-subjects ANOVA, with contrasts within each time bin, bonferroni correction for multiple comparisons).

The bats approached the net opening at a high flight speed. Bats 1 and 2 reduced flight speed as they neared the net opening in all conditions, while bat 3 only reduced flight speed during no-wind condition trials (Fig. 4.5A). Once past the net opening, the bats increased flight speed. Bats flew faster during wind condition trials, with a significant difference occurring between -0.2 - 0.3 seconds after the net crossing (-0.2 - 0.2 seconds $p<0.001$, 0.3 seconds $p=0.001$, number of observations=4881). Bats also flew faster 0.6 seconds after the net crossing ($p=0.044$). Bat 1 flew a maximum difference of 0.44 meters per second faster, bat 2 flew 0.20 meters per second faster, and bat 3 flew 0.52 meters per second faster during the wind condition trials.

Differences in trajectory patterns between bats (Fig. 4.3) resulted in differences in turn rate as they approached the net opening (Fig. 4.5B). Bat 2 had the highest turn rate before crossing the net opening, with a value of 136 +/- 4 degrees per second, while bats

1 and 2 had lower turn rates (maximum values of 117 +- 3 and 98 +/- 3 degrees per second). Turn rate was larger during wind condition trials between 0.2 - 0.4 seconds after net crossing (0.2 - 0.3 seconds $p<0.001$, 0.4 seconds $p=.007$, number of observations=4884). Bat 1 had a maximum difference in turn rate between no-wind and wind conditions of 17 degrees per second, bat 2 had a maximum difference of 30 degrees per second, and bat 3 had a maximum difference of 62 degrees per second.

All three bats had a positive climb rate before the net crossing, but after net crossing, climb rate became negative (diving) (Fig. 4.5C). The climb rate for each bat was larger at time bins -0.2 - 0 seconds before the net crossing during wind condition trials (-0.2 - -0.1 seconds $p<0.001$, 0 seconds $p=0.001$, number of observations=4884). Bat 1 had a maximum climb rate difference of 0.39 meters per second, bat 2 had a difference 0.25 meters per second, and bat 3 had a difference of 0.35 meters per second. After the net crossing, during wind condition trials, the climb rate decreased below the no-wind condition trials between 0.2 - 0.5 seconds after crossing the net opening (0.2 - 0.5 seconds $p<0.001$).

The bats wingbeat rate fluctuated between an average of 10 and 14 Hz as they navigated the net openings (Fig. 4.5D). After crossing the net opening, the bats increased wingbeat rate as they prepared to capture the tethered insect. No significant differences in wingbeat rate between no-wind and wind conditions occurred before the net crossing. After the net crossing, the wingbeat rate increased in no-wind condition trials compared to wind condition at 0.1 seconds after crossing the net ($p<0.001$, number of

observations=4732). Further away from the net crossing, between 0.6 - 0.7 seconds, the bats used a higher wingbeat rate in wind condition trials (0.6 seconds $p<0.001$, 0.7 seconds $p=0.002$).

Each of the bats started at a low elevation in each trial and climbed upwards towards the net opening (Fig. 4.5E). Past the net opening, the bats decreased elevation as they continued on to capture the tethered insect, located 1.61 m above the floor. The net opening tapered at the bottom to a "V" (Fig. 4.1), with the tip at 1.37 meters above the floor, so each of the bats was well above the lower part of the net opening as they crossed the net, at 1.92 +/- 0.04 m, 1.96 +/- 0.03 m, and 1.79 +/- 0.03 m for bats 1, 2, and 3. During wind condition trials, immediately after crossing the net opening, the bats flew at a higher elevation than during no-wind condition trials, with an elevation difference of 0.09 m for bat 1, 0.05 m for bat 2, and 0.05 m for bat 3 (0.1 seconds $p=0.012$, number of observations=4884).

During the net crossing, the absolute value of the horizontal position of the flight trajectories was very close to the center of the opening (Fig. 4.5F). At the time of net crossing (t=0) during no-wind trials, the bats were 0.07 +/- 0.04 m, 0.08 +/- 0.05 m, 0.07 +/- 0.03 m from the center of the net opening. No difference was found in the interaction term so no comparisons between the conditions and the time relative to the net crossing was made (number of observations=4884).

Kinematic measures

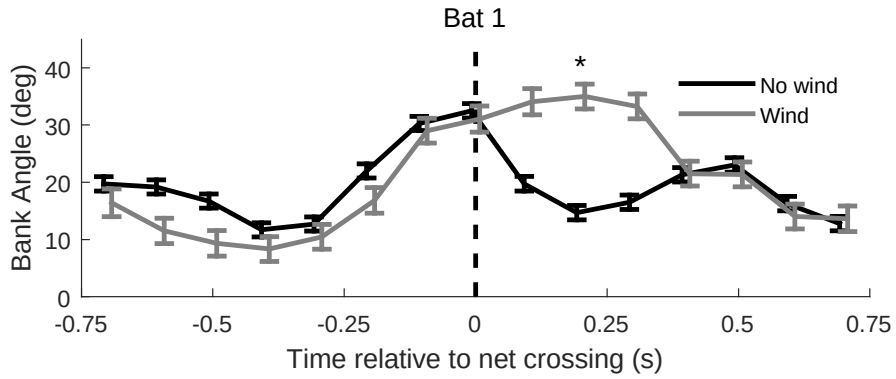

Fig. 4.6: Bank angle for bat 1 relative to net crossing time for no-wind (black) and wind (gray) trial conditions. Values are medians +/- S.E.M. Included in the analysis were 24 trials from the no-wind condition and 21 trials from the wind condition.

We calculated the bank angle as the angle between the left and right wings to the ground (see methods), and compared between no-wind and wind condition trials for bat 1 (Fig. 4.6). Bank angle was relatively stable until 0.3 seconds before net crossing. Bank angle increased as the bat approached the net opening, from an average of 11 degrees to 30 degrees, between 0.3 seconds before net crossing to the net cross time. Between 0.1 and 0.3 seconds after crossing the net opening, the bank angle was larger in wind condition trials than in no-wind condition trials. There was a significant difference between the conditions at 0.2 seconds after net crossing ($p=0.029$, number of observations=638). The maximum difference in bank angle between no-wind and wind conditions after crossing the net opening was 21 degrees.

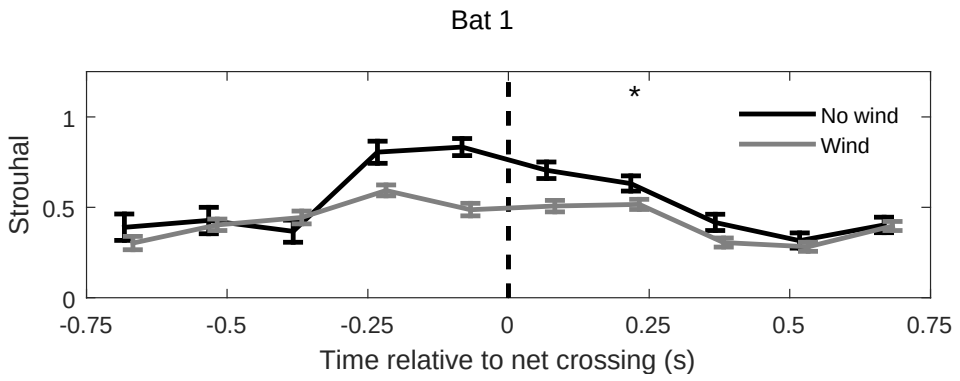

Fig. 4.7: Strouhal number for bat 1 relative to net crossing time for no-wind (black) and wind (gray) trial conditions. Values are medians +/- S.E.M. Strouhal number is presented for both left and right wings. Included in the analysis were 24 trials from the no-wind condition and 21 trials from the wind condition.

For bat 1, we calculated the Strouhal number (*St*), a dimensionless number defined as the wingbeat frequency (*f*) times wingbeat amplitude (*A*) divided by forward flight speed (*U*), which describes oscillating flow mechanisms and predicts the unsteadiness of the flow (Swartz et al., 2012). Unsteady flow becomes crucial outside the range of $0.2 \leq St \leq 0.4$ (Norberg & Winter, 2006). As the bat approached the net opening, we found that *St* increased, from 0.37 +/- 0.06, 0.375 seconds before net crossing, to 0.80 +/- 0.06, 0.225 seconds before net crossing in the no-wind condition (Fig. 4.7). *St* remained large as the bat crossed the net, and decreased steadily until 0.525 seconds after crossing the net, when $St = 0.32$ +/- 0.04. During the wind condition trials, *St* did not increase in value as high as in the no-wind condition, with a maximum value reaching 0.59 +/- 0.03, 0.225 seconds before net crossing. The difference in *St* between the no-wind condition and wind condition was significantly different 0.225 seconds after the net crossing ($p=0.003$, number of observations=277).

Discussion

This study was conducted to investigate the impact of wind gusts on bat flight behavior. Bats navigated a net opening and captured a tethered insect, as they encountered gusts of wind from different directions. Bats successfully navigated the net opening during trials with wind gusts, and they did so by making adjustments in flight behavior, which was quantified with a high-speed motion capture system. The bats exhibited changes in trajectory paths during wind gust trials. In addition, bats showed differences in flight speed, turn rate, climb rate, wingbeat rate, flight elevation and horizontal position between wind and no-wind conditions in relation to the time to net crossing. For one bat, we measured detailed flight kinematics. In these data, we found an increased bank angle during wind condition trials compared to no-wind condition trials, and we also found differences in the Strouhal number between no-wind and wind conditions.

Performance

Under the no-wind condition, the bats navigated the net opening with very few errors, rarely crashing into the net (Fig. 4.2). While net crashes occurred more frequently during wind gusts, the bats showed relatively few crashes even under wind conditions. It appears that bats successfully maneuvered through the net opening under wind conditions by making adjustments in flight trajectory, speed, and wing kinematics, as described below.

Changes in flight trajectories

We found that wind gusts resulted in changes to the bat flight trajectories, which we measured with occupancy histograms (Fig. 4.3), and compared peak and spread between wind and no-wind conditions (Fig. 4.4). We found that the flight paths during the no-wind condition were highly stereotyped, but during wind gust trials, the bats showed more variable flight paths. (Barchi et al., 2013) found that stereotyped flight paths of big brown bats developed over a series of days in an experimental flight room with many obstacles. In the present study, the bat test subjects already had weeks of experience during training with the obstacle net before data recordings, so we could not test for the development of stereotyped flight behavior in this paradigm. However, the wind condition disrupted the stereotyped flight trajectories exhibited in the no-wind condition. It is noteworthy that the bats persisted with stereotyped flight trajectories in the no-wind trials, as they were randomly interspersed with wind gust trials.

Bats slowed their flight speed as they approached the net opening during no-wind trials (Fig. 4.5A). During wind gust trials, the bats flew faster than in trials with no-wind. The difference in flight speed began when the bats first experienced the wind gust, before the net crossing. When encountering wind gusts, the bats may have been unable to slow their flight speed. Slow and maneuvering flight is aerodynamically challenging to generate lift. The wind gusts disrupted the airflow around the bats, creating turbulence, which likely made it more difficult for the bats to fly slowly. Additionally, the bats may have flown faster in order to sustain lift and travel through the wind gust as quickly as possible.

After passing through the net opening, near the time of insect capture, the bats increased turn rate in the wind condition compared to no-wind trials (Fig. 4.5B). The lower turn rate observed during the no-wind trials indicates that path planning during these trials led to more direct flight trajectories. During wind gust trials, bats exhibited more variable flight trajectories (Fig. 4.3). Thus, the increased turn rate, near the time of insect capture, was likely a recovery from the wind gust as bats corrected their trajectories to capture the insect.

Bats exhibited a positive climb rate during the approach to the net crossing and a negative rate after the net crossing (Fig. 4.5C). During trials with the wind gust, climb rate was more positive as bats approached the net opening and more negative at the time of insect capture, compared with the no-wind condition. This change in climb rate resulted in a change in flight elevation after the net crossing time (Fig. 4.5E). Bats in the wind condition showed more extreme values of climb rate, but these did not result in large overall differences in flight elevation between conditions.

Wingbeat rate remained relatively stable during the bats' approach to the net opening, but increased sharply after the net crossing (Fig. 4.5D). During wind gust trials, wingbeat rate was lower after the net crossing, and higher at the end of the trial, after insect capture. Immediately after the net crossing, during wind gust trials, the bats also showed a faster flight speed and a higher elevation, than trials with no-wind. The reduced wingbeat frequency, as a mechanism to reduce thrust and lift, would have resulted in a

decreased flight speed and elevation. This difference in wingbeat rate after the net crossing only persisted for 0.1 seconds.

We found that the bats crossed the net opening very close to the center of the opening, typically within 0.1 m of the center (Fig. 4.5F). The maximum width of the net opening was 0.48 m where the bats passed through, while the maximum wing span recorded from each bat in flight was 0.30 m, 0.29 m, and 0.31 m for bats 1, 2 and 3 respectively. We only analyzed trajectory data from trials without crashes, so in this subset of data we expect to see accurate maneuvers through the net opening. It is noteworthy that the bats showed high accuracy in their maneuvers, under both no-wind and wind conditions. Even with wings outstretched, they would have still had 0.1 m leeway on either side to not hit the net. This indicates that crashes were likely significant errors in path planning in which the bats misjudged the net opening by tens of centimeters.

Banking and turning

We found that changes in bank angle and turn rate occurred together, in time, relative to the net crossing, for bat 1 (Fig. 4.5B, 4.6). Turn rate and bank angle both increased as the bat approached the net opening. After the net crossing, in the no-wind condition, turn rate and bank angle both decreased. In the wind condition, turn rate and bank angle both were larger after the net crossing. The concurrent changes in turn rate and bank angle indicate that the bats used banking to generate turning force. An alternate strategy for turning is crabbed turns, in which the animal rotates in yaw along the vertical axis to produce a lateral force. Iriarte-Díaz & Swartz (2008) found that the frugivorous bat

species, *Cynopterus brachyotis*, used a combination of banked and crabbed turns to complete a low-speed 90 degree turn. In the present study, we were unable to measure heading angle, and thus determining the relative role of banked and crabbed turns was not possible. A future study could examine how wind gusts from different directions modify the preference of a bat to use crabbed or banked turns.

Strouhal during wind gusts

Animals in cruising flight converge on a Strouhal number within a range of 0.2 – 0.4, which is the range favorable for flight force production (Taylor et al., 2003). Force production outside this range can be negatively influenced by unsteady flow (Anderson, Streitlien, Barrett, & Triantafyllou, 1998; Wang, 2000). Previous studies of the hovering, nectar-feeding bat *Glossophaga soricina,* have found *St* values during slow flight outside the preferred range (Norberg & Winter, 2006; Wolf et al., 2010). In present study, we examined the flight of the aerial-hawking insectivorous big brown bat, which is adapted for faster more open space flight than the hovering species *G. soricina*. As the bats in the present study navigated the net opening, they flew at slow flight speeds, between 1.5 and 3 meters per second (Fig. 4.5). The slow flight speed, especially around the time of net crossing during the no-wind condition, resulted in the high *St* values recorded (> 0.8) (Fig. 4.7). In the wind condition, the bats did not lower flight speed to the same extent as they navigated the net. Flight speed differences around the time of the net crossing likely had the largest effect on the difference in *St* value between no-wind and wind conditions. Under the wind condition, the highest average *St* value was 0.59 +/- 0.03, still outside the

preferred range for favorable force production. Bats in wind gusts may not be able to tolerate the additional unsteady flow when flying at slow speeds.

Flight of the big brown bat is remarkably robust. Changes in this animal's flight speed and wing kinematics in response to wind gusts allowed it to maneuver around obstacles and intercept prey under challenging conditions. The big brown bat's adaptive flight behavior contributes to its successful aerial locomotion in the natural environment. Open questions remain about how other species of bats or animals react to wind gusts and how bats sense wind gusts to produce appropriate flight kinematic output.

Acknowledgments

We thank Delphia Varadarajan for assistance with animal training and data collection and Alan Leslie and Dilip Venugopal for assistance with statistical analysis.

Funding

This work was supported by a Comparative and Evolutionary Biology of Hearing T32 predoctoral fellowship to B. Falk from the National Institute of Deafness and Communication Disorders [DC-00046, A. Popper, PI], and the Air Force Office of Scientific Research F49620-01-1-0335 to K. Breuer, PI, and IFA95§O-14-1-0398 to T. Daniel, PI, with subcontracts to C. Moss].

Chapter 5: Future directions

This thesis was composed of three studies on the echolocating big brown bat, *Eptesicus fuscus*. In the first study, bats were tested in two different environments, an open space and a cluttered space. Bats were found to adjust both flight and echolocation parameters to the environment. In the second study, we characterized changes to flight and sonar behavior as bats made sharp turns and steep climbs through a net obstacle. In the third study, we tested how bats reacted to gusts of wind while navigating through a narrow net opening. Together, these studies broaden our understanding of how bats adapt their behavior and how they coordinate flight and sonar behavior together in order to perform across varied environments.

The motion tracking cameras

For studies 2 and 3, a motion capture (Vicon) system was used to collect position information on the bats. These experiments were some of the first in the batlab to use this system. The motion tracking system works through capturing video across multiple cameras (we used 10 in these studies). Each camera records and sends only what is observed above a threshold. Those data are sent in real time to a central processing unit (Vicon giganet). The values sent by each camera are combined into 3D points, through Vicon's algorithms, which are similar, if not the same, as the DLT algorithm (Shapiro, 1978). The motion tracking system has capabilities that our previous high-speed camera system lacked (2 Photron FASTCAM PCI R2 cameras which recorded 512x480 resolution images at up to 250 Hz). The recordings of the motion tracking system are not

limited by a buffer, so they can continue recording for an unlimited time (only limitation is hard drive space). Because data recorded has to be above a threshold, the cameras function using reflective markers, which return high intensity reflections. The Vicon system can also record at a higher frame rate, up to 370 Hz, without reducing resolution. It also reflective markers on the bats wings, which allow the study of 3D flight kinematics in a large volume.

A number of limitations to the Vicon system became evident once in use. Initially, the software for collecting data was extremely unstable. Software updates eventually resolved those issues, but crashes during data collection were frequent in these first experiments. The 3D data generated by the Vicon software (Nexus) contained extra 3D points that were not actually present, termed "phantom" points. These points were generated as reflections recorded on one camera and were attributed to reflections on another camera, but, in actuality, these were two separate reflections which should not have been joined to create a 3D point. A separate issue was point drop outs, in which reflective markers were not tracked through the entire wingbeat. This phenomenon was common in the data collected in the studies in this thesis. Labeling of the individual 3D points is necessary in order to make kinematic measurements. However, these two problems, point drop outs and phantom points, created a hurdle which the built-in, Vicon provided, labeling software could not overcome. The labeling model required points from all the different reflective markers over time in order to label any of the markers. For this issue, the drop outs were more problematic than the phantom points. Reflections under the threshold on each camera was not recorded at all, which can reduce phantom

points, but also had significant consequences to labeling or 3D track reconstruction. The cameras were also significantly less wide-angle than the previous system, so recording flight trajectories along the edge of the room is very difficult. The big brown bat typically makes circular paths around the edge of the flight room, unless capturing an insect, so the recording system can miss large portions of flight trajectories if the experiment is not designed with that in mind. Some of these limitations were resolved using custom built software in Matlab to do the labeling (Falk, 2015). However, many of these issues remain.

Proposed future experiments

In future experiments, using a different type of reflective marker on the wing could allow better 3D reconstruction and fewer drop outs. The reflective tape used on the wings of the bats is not invasive and does not disturb the bats, while it also provides the cameras a target to track. We place the tape on both sides of the wing, so that the markers are visible whether the wing is raised or lowered. However, as the markers are planer pieces of tape, they reflect directionally to the cameras, and thus multiple cameras often cannot view the same reflective marker, a requirement for 3D reconstruction. Another possibility for wing markers would be raised domes of reflective tape, which could be glued to the surface of the wings and would provide a more omnidirectional reflection. Previous attempts to use these types of markers on the wings failed, because the markers can be removed by the bats and they can also interfere with the bat flight. However, adjustments to the size of the markers and the adhesive could make these a viable replacement to the flat tape markers. Another possibility is to use a light source, perhaps

miniaturized LEDs, glued onto the wing, which would generate light to be captured by the camera system. Instead having to reflect light from each marker, a direct transmission from the wing to the cameras could be more robust. Powering the light source would be the primary difficult, but perhaps could be achieved though small batteries attached to each LED. Finally, additional cameras could allow for more reflections to be recorded, as cameras placed directly above or below the bat could record from angles which previously would have been not viewable.

Detailed flight kinematic analyses of bats performing complex aerial maneuvers are only just becoming possible. Previous studies have used high-speed cameras to image small volumes of space and track markers placed on the wings and body of the bat. Advancements in video technology have reduced the price of high-speed cameras and have allowed recordings at higher resolution and high frame rates. Higher resolution cameras allow tracking in a larger volume, as more detail can be extracted from the images at further distances to the camera. Motion-tracking systems allow for larger volumes to be captured using camera arrays. By utilizing these new techniques, measures of flight kinematics can be made while the bats perform sharp turns and make steep climbs, or make other aerial maneuvers. A full characterization of the changes in wing shape during maneuvering would allow a more thorough understanding of how bats generate lift forces during these maneuvers. The camber, or wing curvature, and wing area could be calculated with a few additional markers placed on the wing. Riskin et al. (2008) report that markers along digit 3 and 4 provide the highest dimensional complexity and detail which markers would be necessary. The stroke plane angle, the

angle between the forward axis and the wing's path through the lateral plane, is a measure of the angle of attack during flapping flight. The camber, wing area, and stroke plane angle have large impacts on the lift force and can be adjusted in flight by the bat. Additional measures that could be advantageous are the downstroke ratio, or the ratio of the downstroke to the wingbeat period, and the extent that the bats tuck or spread their wings. Measures of the lift coefficient and lift force during maneuvers would be valuable to understand the role of unsteady forces during flapping flight. Measurement of the asymmetry between wing movements in markers could provide details on how the bats generate turns.

One unstudied bat flight kinematic phenomenon is insect capture. Insectivorous bats scoop the insect into their tail and wing membranes. During the capture behavior, they cease flapping flight and lose altitude. After the insect capture, they recover and continue flying, while manipulating the insect. Studying the dynamics of this behavior could inform how bats recover in stall situations.

Microscopic hairs on the bat's wings contribute sensory information to adaptive flight behaviors. The wing hairs are hypothesized to provide the flying bat with sensory information about air currents across the wing membrane. Neurophysiological studies have shown that bat wing hairs are directionally sensitive to airflow, and behavioral studies have shown that wing hair removal results in a decrease in the bat's flight maneuverability (Sterbing-D'Angelo et al., 2011). One expansion of the study on wind gusts could be a study of the effects of air turbulence on wingbeat kinematics, flight path,

and echolocation behavior in bats with and without wing hairs. Reaction times, recovery from the wind gust, and crash performance could be compared in bats with and without wing hairs. Is there evidence for behavioral decisions being made based on the presence or absence of wing hairs?

All of the studies in this thesis have been on the big brown bat, *Eptesicus fuscus*. A comparative approach, examining the coordination of flight and sonar behaviors across species of bats, would yield information about the diversity of adaptive behaviors. The few species studied for detailed flight kinematics represent a very small portion of the total number of bats (including the data in this thesis, 5 species total out of over 1200). Expanding the number of species studied for detailed flight kinematics to *Carollia perspicillata*, would enable comparisons to a genus not previously studied, and to a species which emits very different type of sonar call than *E. fuscus*, higher in frequency, more directional, and with sound emissions which originate from the nose and mouth. In addition, *C. perspicillata* is a highly maneuverable species, which allows the study of maneuvering flight in the lab.

Recent advances in technology have miniaturized telemetry and data logging systems, which can be used to record the bat in its natural environment by attaching a "backpack" to the bat (Cvikel, Egert Berg, et al., 2015; Cvikel, Levin, et al., 2015). Using GPS coordinate recordings with vocal behavior, a researcher can ask questions that are not possible in the lab. One example would be a comparison of the flight trajectories, using GPS coordinates, of bats with and without wing hairs. Another comparison could be

between bat flight trajectories on windy and still nights to observe how they adapt in the wild. The varied strategies bats use could quite different from the behaviors observed in the lab.

Summary

The results from the studies in this thesis detail the big brown bat's coordination of flight and sonar behaviors with adaptations to different experimental conditions. These studies expand our knowledge of the bat's flight and echolocation behavior. Bats adapt the shape and movement of the wing in complex ways to produce appropriate aerodynamic forces which vary from one wingbeat to the next. Bats also adjust the production and signal design of echolocation behavior to meet varied task demands. Through the examination of flight motor output and sonar behavior, we can better understand sensorimotor integration.

References

Aldridge, H. D. J. N. (1986). Kinematics and Aerodynamics of the Greater Horseshoe Bat, *Rhinolophus Ferrumequinum*, in Horizontal Flight at Various Flight Speeds. *Journal of Experimental Biology*, *126*(1), 479–497.

Aldridge, H. D. J. N. (1987). Turning flight of bats. *Journal of Experimental Biology*, *128*(1), 419–425.

Alexander, D. (2002). *Nature's flyers : birds, insects, and the biomechanics of flight*. Baltimore: Johns Hopkins University Press.

Aloimonos, J., Weiss, I., & Bandyopadhyay, A. (1988). Active vision. *International Journal of Computer Vision*, *1*(4), 333–356. http://doi.org/10.1007/BF00133571

Anderson, J. M., Streitlien, K., Barrett, D. S., & Triantafyllou, M. S. (1998). Oscillating foils of high propulsive efficiency. *Journal of Fluid Mechanics*, *360*, 41–72. http://doi.org/10.1017/S0022112097008392

Au, W. W. L. (1993). *The Sonar of Dolphins*. Springer Science & Business Media.

Barchi, J. R., Knowles, J. M., & Simmons, J. A. (2013). Spatial memory and stereotypy of flight paths by big brown bats in cluttered surroundings. *The Journal of Experimental Biology*, *216*(6), 1053–1063. http://doi.org/10.1242/jeb.073197

Bell, G. P., & Fenton, M. B. (1984). The use of Doppler-shifted echoes as a flutter detection and clutter rejection system: the echolocation and feeding behavior of

Hipposideros ruber (Chiroptera: Hipposideridae). *Behavioral Ecology and Sociobiology*, *15*(2), 109–114. http://doi.org/10.1007/BF00299377

Berens, P. (2009). CircStat: a MATLAB toolbox for circular statistics. *J Stat Softw*, *31*(10), 1–21.

Bininda-Emonds, O. R. P., & Russell, A. P. (1994). Flight style in bats as predicted from wing morphometry: the effects of specimen preservation. *Journal of Zoology*, *234*(2), 275–287. http://doi.org/10.1111/j.1469-7998.1994.tb06075.x

Brinkløv, S., Fenton, M. B., & Ratcliffe, J. M. (2013). Echolocation in Oilbirds and swiftlets. *Frontiers in Physiology*, *4*. http://doi.org/10.3389/fphys.2013.00123

Cahlander, D. A., McCue, J. J. G., & Webster, F. A. (1964). The Determination of Distance by Echolocating Bats. *Nature*, *201*(4919), 544–546. http://doi.org/10.1038/201544a0

Catania, K. C., & Henry, E. C. (2006). Touching on somatosensory specializations in mammals. *Current Opinion in Neurobiology*, *16*(4), 467–473. http://doi.org/10.1016/j.conb.2006.06.010

Crawford, R. L., & Baker, W. W. (1981). Bats Killed at a North Florida Television Tower: A 25-Year Record. *Journal of Mammalogy*, *62*(3), 651–652. http://doi.org/10.2307/1380421

Cvikel, N., Egert Berg, K., Levin, E., Hurme, E., Borissov, I., Boonman, A., … Yovel, Y. (2015). Bats Aggregate to Improve Prey Search but Might Be Impaired when Their Density Becomes Too High. *Current Biology*. http://doi.org/10.1016/j.cub.2014.11.010

Cvikel, N., Levin, E., Hurme, E., Borissov, I., Boonman, A., Amichai, E., & Yovel, Y. (2015). On-board recordings reveal no jamming avoidance in wild bats. *Proceedings of the Royal Society of London B: Biological Sciences*, *282*(1798), 20142274. http://doi.org/10.1098/rspb.2014.2274

Diamond, M. E., von Heimendahl, M., Knutsen, P. M., Kleinfeld, D., & Ahissar, E. (2008). "Where" and "what" in the whisker sensorimotor system. *Nature Reviews. Neuroscience*, *9*(8), 601–612. http://doi.org/10.1038/nrn2411

Ellington, C. P., van den Berg, C., Willmott, A. P., & Thomas, A. L. R. (1996). Leading-edge vortices in insect flight. *Nature*, *384*(6610), 626–630. http://doi.org/10.1038/384626a0

Falk, B. (2015). *viconLabeler*. Retrieved from https://github.com/falkben/viconLabeler

Falk, B., Jakobsen, L., Surlykke, A., & Moss, C. F. (2014). Bats coordinate sonar and flight behavior as they forage in open and cluttered environments. *The Journal of Experimental Biology*, *217*(24), 4356–4364. http://doi.org/10.1242/jeb.114132

Falk, B., Williams, T., Aytekin, M., & Moss, C. F. (2011). Adaptive behavior for texture discrimination by the free-flying big brown bat, *Eptesicus fuscus*. *Journal of Comparative Physiology A*, *197*(5), 491–503. http://doi.org/10.1007/s00359-010-0621-6

Farney, J., & Fleharty, E. D. (1969). Aspect Ratio, Loading, Wing Span, and Membrane Areas of Bats. *Journal of Mammalogy*, *50*(2), 362–367. http://doi.org/10.2307/1378361

Faure, P. A., & Barclay, R. M. (1994). Substrate-gleaning versus aerial-hawking: plasticity in the foraging and echolocation behaviour of the long-eared bat, *Myotis evotis*. *Journal of Comparative Physiology. A, Sensory, Neural, and Behavioral Physiology*, *174*(5), 651–660.

Gelder, R. G. V. (1956). Echo-Location Failure in Migratory Bats. *Transactions of the Kansas Academy of Science (1903-)*, *59*(2), 220–222. http://doi.org/10.2307/3626963

Ghose, K., & Moss, C. F. (2003). The sonar beam pattern of a flying bat as it tracks tethered insects. *The Journal of the Acoustical Society of America*, *114*(2), 1120–1131. http://doi.org/10.1121/1.1589754

Ghose, K., & Moss, C. F. (2006). Steering by Hearing: A Bat's Acoustic Gaze Is Linked to Its Flight Motor Output by a Delayed, Adaptive Linear Law. *J. Neurosci.*, *26*(6), 1704–1710. http://doi.org/10.1523/JNEUROSCI.4315-05.2006

Griffin, D. R. (1958). *Listening in the Dark*. Yale University Press New Haven.

Hartley, D. J. (1992). Stabilization of perceived echo amplitudes in echolocating bats. I. Echo detection and automatic gain control in the big brown bat, *Eptesicus fuscus*, and the fishing bat, *Noctilio leporinus*. *The Journal of the Acoustical Society of America*, *91*(2), 1120. http://doi.org/10.1121/1.402639

Hartley, D. J., & Suthers, R. A. (1989). The sound emission pattern of the echolocating bat, *Eptesicus fuscus*. *The Journal of the Acoustical Society of America*, *85*(3), 1348–1351. http://doi.org/10.1121/1.397466

Hartridge, H. (1945). Acoustic Control in the Flight of Bats. *Nature*, *156*(3965), 490–494. http://doi.org/10.1038/156490a0

Hedenström, A., & Johansson, L. C. (2015). Bat flight: aerodynamics, kinematics and flight morphology. *The Journal of Experimental Biology*, *218*(5), 653–663. http://doi.org/10.1242/jeb.031203

Hedenström, A., Johansson, L. C., Wolf, M., von Busse, R., Winter, Y., & Spedding, G. R. (2007). Bat Flight Generates Complex Aerodynamic Tracks. *Science*, *316*(5826), 894–897. http://doi.org/10.1126/science.1142281

Hedrick, T. L., Cheng, B., & Deng, X. (2009). Wingbeat Time and the Scaling of Passive Rotational Damping in Flapping Flight. *Science*, *324*(5924), 252–255. http://doi.org/10.1126/science.1168431

Hiryu, S., Bates, M. E., Simmons, J. A., & Riquimaroux, H. (2010). FM echolocating bats shift frequencies to avoid broadcast-echo ambiguity in clutter. *Proceedings of the National Academy of Sciences of the United States of America*, *107*(15), 7048–7053. http://doi.org/10.1073/pnas.1000429107

Hiryu, S., Hagino, T., Riquimaroux, H., & Watanabe, Y. (2007). Echo-intensity compensation in echolocating bats (*Pipistrellus abramus*) during flight measured by a

telemetry microphone. *The Journal of the Acoustical Society of America*, *121*(3), 1749–1757. http://doi.org/10.1121/1.2431337

Holderied, M. W., Korine, C., Fenton, M. B., Parsons, S., Robson, S., & Jones, G. (2005). Echolocation call intensity in the aerial hawking bat *Eptesicus bottae* (Vespertilionidae) studied using stereo videogrammetry. *The Journal of Experimental Biology*, *208*(7), 1321–1327. http://doi.org/10.1242/jeb.01528

Holland, R. A., Waters, D. A., & Rayner, J. M. V. (2004). Echolocation signal structure in the Megachiropteran bat Rousettus aegyptiacus Geoffroy 1810. *Journal of Experimental Biology*, *207*(25), 4361–4369. http://doi.org/10.1242/jeb.01288

Hubel, T. Y., Hristov, N. I., Swartz, S. M., & Breuer, K. S. (2012). Changes in kinematics and aerodynamics over a range of speeds in *Tadarida brasiliensis*, the Brazilian free-tailed bat. *Journal of The Royal Society Interface*, *9*(71), 1120–1130. http://doi.org/10.1098/rsif.2011.0838

Hubel, T. Y., Hristov, N., Swartz, S., & Breuer, K. (2009). Time-resolved wake structure and kinematics of bat flight. *Experiments in Fluids*, *46*(5), 933–943. http://doi.org/10.1007/s00348-009-0624-7

Hubel, T. Y., Riskin, D. K., Swartz, S. M., & Breuer, K. S. (2010). Wake Structure and Wing Kinematics: The Flight of the Lesser Dog-Faced Fruit Bat, *Cynopterus Brachyotis*. *Journal of Experimental Biology*, *213*(20), 3427–3440. http://doi.org/10.1242/jeb.043257

IÄřbus, A. L. (1967). *Eye movements and vision.* (L. A. Rigss, Ed.). New York: Plenum Press.

Iriarte-Díaz, J., & Swartz, S. M. (2008). Kinematics of slow turn maneuvering in the fruit bat *Cynopterus brachyotis*. *Journal of Experimental Biology*, *211*(21), 3478–3489. http://doi.org/10.1242/jeb.017590

Jakobsen, L., Ratcliffe, J. M., & Surlykke, A. (2013). Convergent acoustic field of view in echolocating bats. *Nature*, *493*(7430), 93–96. http://doi.org/10.1038/nature11664

Jakobsen, L., & Surlykke, A. (2010). Vespertilionid bats control the width of their biosonar sound beam dynamically during prey pursuit. *Proceedings of the National Academy of Sciences*, *107*(31), 13930–13935. http://doi.org/10.1073/pnas.1006630107

Jensen, M. E., & Miller, L. A. (1999). Echolocation signals of the bat *Eptesicus serotinus* recorded using a vertical microphone array: effect of flight altitude on searching signals. *Behavioral Ecology and Sociobiology*, *47*(1-2), 60–69. http://doi.org/10.1007/s002650050650

Jensen, M. E., Moss, C. F., & Surlykke, A. (2005). Echolocating bats can use acoustic landmarks for spatial orientation. *The Journal of Experimental Biology*, *208*(Pt 23), 4399–4410. http://doi.org/10.1242/jeb.01901

Johnson, J. B., Gates, J. E., & Zegre, N. P. (2010). Monitoring seasonal bat activity on a coastal barrier island in Maryland, USA. *Environmental Monitoring and Assessment*, *173*(1-4), 685–699. http://doi.org/10.1007/s10661-010-1415-6

Jones, G., & Teeling, E. C. (2006). The evolution of echolocation in bats. *Trends in Ecology & Evolution*, *21*(3), 149–156. http://doi.org/10.1016/j.tree.2006.01.001

Kalko, E. K. V., & Schnitzler, H.-U. (1989). The echolocation and hunting behavior of Daubenton's bat, *Myotis daubentoni*. *Behavioral Ecology and Sociobiology*, *24*(4), 225–238. http://doi.org/10.1007/BF00295202

Kalko, E. K. V., & Schnitzler, H.-U. (1993). Plasticity in Echolocation Signals of European Pipistrelle Bats in Search Flight: Implications for Habitat Use and Prey Detection. *Behavioral Ecology and Sociobiology*, *33*(6), 415–428.

Koblitz, J. C., Stilz, P., & Schnitzler, H.-U. (2010). Source levels of echolocation signals vary in correlation with wingbeat cycle in landing big brown bats (*Eptesicus fuscus*). *The Journal of Experimental Biology*, *213*(Pt 19), 3263–3268. http://doi.org/10.1242/jeb.045450

Kothari, N. B., Wohlgemuth, M. J., Hulgard, K., Surlykke, A., & Moss, C. F. (2014). Timing matters: sonar call groups facilitate target localization in bats. *Integrative Physiology*, *5*, 168. http://doi.org/10.3389/fphys.2014.00168

Mitchinson, B., Grant, R. A., Arkley, K., Rankov, V., Perkon, I., & Prescott, T. J. (2011). Active vibrissal sensing in rodents and marsupials. *Philosophical Transactions of the Royal Society B: Biological Sciences*, *366*(1581), 3037–3048. http://doi.org/10.1098/rstb.2011.0156

Moss, C. F., Bohn, K., Gilkenson, H., & Surlykke, A. (2006). Active Listening for Spatial Orientation in a Complex Auditory Scene. *PLoS Biology*, *4*(4), 615–626. http://doi.org/10.1371/journal.pbio.0040079

Moss, C. F., Chiu, C., & Surlykke, A. (2011). Adaptive vocal behavior drives perception by echolocation in bats. *Current Opinion in Neurobiology*, *21*(4), 645–652. http://doi.org/10.1016/j.conb.2011.05.028

Moss, C. F., & Surlykke, A. (2001). Auditory scene analysis by echolocation in bats. *The Journal of the Acoustical Society of America*, *110*(4), 2207–2226. http://doi.org/10.1121/1.1398051

Moss, C. F., & Surlykke, A. (2010). Probing the natural scene by echolocation in bats. *Frontiers in Behavioral Neuroscience*, *4*, 33. http://doi.org/10.3389/fnbeh.2010.00033

Muijres, F. T., Johansson, L. C., Barfield, R., Wolf, M., Spedding, G. R., & Hedenström, A. (2008). Leading-edge vortex improves lift in slow-flying bats. *Science (New York, N.Y.)*, *319*(5867), 1250–1253. http://doi.org/10.1126/science.1153019

Muijres, F. T., Johansson, L. C., Winter, Y., & Hedenström, A. (2011). Comparative Aerodynamic Performance of Flapping Flight in Two Bat Species Using Time-Resolved Wake Visualization. *Journal of The Royal Society Interface*. http://doi.org/10.1098/rsif.2011.0015

Muijres, F. T., Johansson, L. C., Winter, Y., & Hedenström, A. (2014). Leading edge vortices in lesser long-nosed bats occurring at slow but not fast flight speeds. *Bioinspiration & Biomimetics*, *9*(2), 025006. http://doi.org/10.1088/1748-3182/9/2/025006

Neuweiler, G. (2000). *The biology of bats*. Oxford University Press US.

Nicholson, C. P., Tankersley Jr, R. D., Fiedler, J. K., & Nicholas, N. (2005). Assessment and prediction of bird and bat mortality at wind energy facilities in the southeastern United States. *Final Report. Tennessee Valley Authority, Knoxville, Tennessee*.

Norberg, U. M. L. (1970). Hovering flight of *Plecotus auritus linnaeus*. *Bijdragen Tot de Dierkunde*, *40*, 62–66.

Norberg, U. M. L. (1972). Functional osteology and myology of the wing of the dog-faced bat *Rousettus aegyptiacus* (É. Geoffroy) (Mammalia, Chiroptera). *Zoomorphology*, *73*(1), 1–44. http://doi.org/10.1007/BF00418146

Norberg, U. M. L. (1976a). Aerodynamics, Kinematics, and Energetics of Horizontal Flapping Flight in the Long-Eared Bat *Plecotus Auritus*. *The Journal of Experimental Biology*, *65*(1), 179–212.

Norberg, U. M. L. (1976b). Aerodynamics of Hovering Flight in the Long-Eared Bat *Plecotus Auritus*. *The Journal of Experimental Biology*, *65*(2), 459–470.

Norberg, U. M. L. (1990). *Vertebrate flight : mechanics, physiology, morphology, ecology and evolution*. Berlin; New York: Springer-Verlag.

Norberg, U. M. L., & Rayner, J. M. V. (1987). Ecological Morphology and Flight in Bats (Mammalia; Chiroptera): Wing Adaptations, Flight Performance, Foraging Strategy and Echolocation. *Philosophical Transactions of the Royal Society of London. Series B, Biological Sciences*, *316*(1179), 335–427.

Norberg, U. M. L., & Winter, Y. (2006). Wing Beat Kinematics of a Nectar-Feeding Bat, *Glossophaga Soricina*, Flying at Different Flight Speeds and Strouhal Numbers. *Journal of Experimental Biology*, *209*(19), 3887–3897. http://doi.org/10.1242/jeb.02446

O'Farrell, M. J., & Bradley, W. G. (1970). Activity Patterns of Bats over a Desert Spring. *Journal of Mammalogy*, *51*(1), 18–26. http://doi.org/10.2307/1378527

Pennycuick, C. J. (1968). Power Requirements for Horizontal Flight in the Pigeon Columba Livia. *Journal of Experimental Biology*, *49*(3), 527–555.

Petrites, A. E., Eng, O. S., Mowlds, D. S., Simmons, J. A., & DeLong, C. M. (2009). Interpulse interval modulation by echolocating big brown bats (*Eptesicus fuscus*) in different densities of obstacle clutter. *Journal of Comparative Physiology. A, Neuroethology, Sensory, Neural, and Behavioral Physiology*, *195*(6), 603–617. http://doi.org/10.1007/s00359-009-0435-6

Racey, P. A., & Swift, S. M. (1985). Feeding Ecology of *Pipistrellus pipistrellus* (Chiroptera: Vespertilionidae) during Pregnancy and Lactation. I. Foraging Behaviour. *Journal of Animal Ecology*, *54*(1), 205–215. http://doi.org/10.2307/4631

Rayner, J. M. V., & Aldridge, H. D. J. N. (1985). Three-Dimensional Reconstruction of Animal Flight Paths and the Turning Flight of Microchiropteran Bats. *Journal of Experimental Biology*, *118*(1), 247–265.

Reinschmidt, C., & Bogert, T. van den. (1997). KineMat: a MATLAB toolbox for three-dimensional kinematic analyses (Version 1.0). Human Performance Laboratory, University of Calgary. Retrieved from http://isbweb.org/software/movanal/kinemat/

Rice, C. E. (1967). Human Echo Perception. *Science*, *155*(3763), 656–664.

Riskin, D. K., Willis, D. J., Iriarte-Díaz, J., Hedrick, T. L., Kostandov, M., Chen, J., … Swartz, S. M. (2008). Quantifying the complexity of bat wing kinematics. *Journal of Theoretical Biology*, *254*(3), 604–615. http://doi.org/10.1016/j.jtbi.2008.06.011

Russ, J. M., Briffa, M., & Montgomery, W. I. (2003). Seasonal patterns in activity and habitat use by bats (*Pipistrellus* spp. and *Nyctalus leisleri*) in Northern Ireland, determined using a driven transect. *Journal of Zoology*, *259*(3), 289–299. http://doi.org/10.1017/S0952836902003254

Sändig, S., Schnitzler, H.-U., & Denzinger, A. (2014). Echolocation behaviour of the big brown bat (*Eptesicus fuscus*) in an obstacle avoidance task of increasing difficulty. *The Journal of Experimental Biology*, *217*(16), 2876–2884. http://doi.org/10.1242/jeb.099614

Schnitzler, H.-U. (1968). Die Ultraschall-Ortungslaute der Hufeisen-Fledermäuse (Chiroptera-Rhinolophidae) in verschiedenen Orientierungssituationen. *Journal of Comparative Physiology A: Neuroethology, Sensory, Neural, and Behavioral Physiology*, *57*(4), 376–408. http://doi.org/10.1007/BF00303062

Schnitzler, H.-U. (1971). Fledermäuse im Windkanal. *Zeitschrift für vergleichende Physiologie*, *73*(2), 209–221. http://doi.org/10.1007/BF00304133

Schnitzler, H.-U., & Kalko, E. K. V. (2001). Echolocation by Insect-Eating Bats. *BioScience*, *51*(7), 557–569. http://doi.org/10.1641/0006-3568(2001)051[0557:EBIEB]2.0.CO;2

Schnitzler, H.-U., Kalko, E., Miller, L., & Surlykke, A. (1987). The echolocation and hunting behavior of the bat, *Pipistrellus kuhli*. *Journal of Comparative Physiology A*, *161*(2), 267–274. http://doi.org/10.1007/BF00615246

Seibert, A.-M., Koblitz, J. C., Denzinger, A., & Schnitzler, H.-U. (2013). Scanning Behavior in Echolocating Common Pipistrelle Bats (*Pipistrellus pipistrellus*). *PLoS ONE*, *8*(4), e60752. http://doi.org/10.1371/journal.pone.0060752

Shapiro, R. (1978). Direct linear transformation method for three-dimensional cinematography. *Research Quarterly. American Alliance for Health, Physical Education and Recreation*, *49*(2), 197–205.

Shimozawa, T., Suga, N., Hendler, P., & Schuetze, S. (1974). Directional Sensitivity of Echolocation System in Bats Producing Frequency-Modulated Signals. *Journal of Experimental Biology*, *60*(1), 53–69.

Simmons, J. A. (1969). Acoustic Radiation Patterns for the Echolocating Bats *Chilonycteris rubiginosa* and *Eptesicus fuscus*. *The Journal of the Acoustical Society of America*, *46*(4B), 1054–1056. http://doi.org/10.1121/1.1911804

Simmons, J. A. (1973). The resolution of target range by echolocating bats. *The Journal of the Acoustical Society of America*, *54*(1), 157–173. http://doi.org/10.1121/1.1913559

Simmons, J. A., Eastman, K. M., Horowitz, S. S., O'Farrell, M. J., & Lee, D. N. (2001). Versatility of biosonar in the big brown bat, *Eptesicus fuscus*. *Acoustics Research Letters Online*, *2*(1), 43–48. http://doi.org/10.1121/1.1352717

Simmons, J. A., Kick, S. A., Lawrence, B. D., Hale, C., Bard, C., & Escudié, B. (1983). Acuity of horizontal angle discrimination by the echolocating bat, *Eptesicus fuscus*. *Journal of Comparative Physiology*, *153*(3), 321–330. http://doi.org/10.1007/BF00612586

Simmons, J. A., Kick, S. A., Moffat, A. J. M., Masters, W. M., & Kon, D. (1988). Clutter interference along the target range axis in the echolocating bat, *Eptesicus fuscus*. *The Journal of the Acoustical Society of America*, *84*(2), 551–559. http://doi.org/10.1121/1.396832

Simmons, N. B. (2005). Order chiroptera. In D. E. Wilson & D. M. Reeder (Eds.), *Mammal species of the world: a taxonomic and geographic reference* (3rd ed., pp. 312–529). Retrieved from http://www.departments.bucknell.edu/biology/resources/msw3

Speakman, J. R., Anderson, M. E., & Racey, P. A. (1989). The energy cost of echolocation in pipistrelle bats (*Pipistrettus pipistrellus*). *Journal of Comparative Physiology A*, *165*(5), 679–685. http://doi.org/10.1007/BF00610999

Speakman, J. R., & Racey, P. A. (1991). No cost of echolocation for bats in flight. *Nature*, *350*(6317), 421–423. http://doi.org/10.1038/350421a0

Staudacher, E. M., Gebhardt, M., & Dürr, V. (2005). Antennal movements and mechanoreception: neurobiology of active tactile sensors. In *Advances in insect physiology* (Vol. 32, pp. 49–205). Retrieved from http://www.sciencedirect.com/science/article/pii/S0065280605320029/pdf?

md5=9d7aff655ae859f00d421c8b11a1a7e8&pid=1-s2.0-S0065280605320029-main.pdf&_valck=1

Sterbing-D'Angelo, S., Chadha, M., Chiu, C., Falk, B., Xian, W., Barcelo, J., … Moss, C. F. (2011). Bat wing sensors support flight control. *Proceedings of the National Academy of Sciences*. http://doi.org/10.1073/pnas.1018740108

Stroffregen, T. A., & Pittenger, J. B. (1995). Human Echolocation as a Basic Form of Perception and Action. *Ecological Psychology*, *7*(3), 181–216. http://doi.org/10.1207/s15326969eco0703_2

Strother, G. K., & Mogus, M. (1970). Acoustical Beam Patterns for Bats: Some Theoretical Considerations. *The Journal of the Acoustical Society of America*, *48*(6B), 1430–1432. http://doi.org/10.1121/1.1912304

Surlykke, A., Ghose, K., & Moss, C. F. (2009). Acoustic scanning of natural scenes by echolocation in the big brown bat, *Eptesicus fuscus*. *J Exp Biol*, *212*(7), 1011–1020. http://doi.org/10.1242/jeb.024620

Surlykke, A., & Kalko, E. K. V. (2008). Echolocating bats cry out loud to detect their prey. *PloS One*, *3*(4), e2036. http://doi.org/10.1371/journal.pone.0002036

Surlykke, A., Miller, L. A., Møhl, B., Andersen, B. B., Christensen-Dalsgaard, J., & Jørgensen, M. B. (1993). Echolocation in two very small bats from Thailand *Craseonycteris thonglongyai* and *Myotis siligorensis*. *Behavioral Ecology and Sociobiology*, *33*(1), 1–12. http://doi.org/10.1007/BF00164341

Surlykke, A., & Moss, C. F. (2000). Echolocation behavior of big brown bats, *Eptesicus fuscus*, in the field and the laboratory. *The Journal of the Acoustical Society of America*, *108*(5), 2419. http://doi.org/10.1121/1.1315295

Suthers, R. A., Thomas, S. P., & Suthers, B. J. (1972). Respiration, Wing-Beat and Ultrasonic Pulse Emission in an Echo-Locating Bat. *Journal of Experimental Biology*, *56*(1), 37–48.

Swartz, S. M. (1997). Allometric patterning in the limb skeleton of bats: Implications for the mechanics and energetics of powered flight. *Journal of Morphology*, *234*(3), 277–294.

Swartz, S. M., Iriarte-Díaz, J., Riskin, D. K., & Breuer, K. S. (2012). A bird? A plane? No, it's a bat: an introduction to the biomechanics of bat flight. In *Evolutionary History of Bats*. Cambridge University Press.

Taylor, G. K., Nudds, R. L., & Thomas, A. L. R. (2003). Flying and swimming animals cruise at a Strouhal number tuned for high power efficiency. *Nature*, *425*(6959), 707–711. http://doi.org/10.1038/nature02000

Thomas, S. P. (1975). Metabolism during flight in two species of bats, *Phyllostomus hastatus* and *Pteropus gouldii*. *The Journal of Experimental Biology*, *63*(1), 273–293.

Tian, X., Iriarte-Díaz, J., Middleton, K., Galvao, R., Israeli, E., Roemer, A., … Breuer, K. (2006). Direct measurements of the kinematics and dynamics of bat flight. *Bioinspiration & Biomimetics*, *1*(4), S10–18. http://doi.org/10.1088/1748-3182/1/4/S02

Triantafyllou, G. S., Triantafyllou, M. S., & Grosenbaugh, M. A. (1993). Optimal Thrust Development in Oscillating Foils with Application to Fish Propulsion. *Journal of Fluids and Structures*, *7*(2), 205–224. http://doi.org/10.1006/jfls.1993.1012

Triantafyllou, M. S., Triantafyllou, G. S., & Gopalkrishnan, R. (1991). Wake mechanics for thrust generation in oscillating foils. *Physics of Fluids A: Fluid Dynamics (1989-1993)*, *3*(12), 2835–2837. http://doi.org/10.1063/1.858173

Von Busse, R., Hedenström, A., Winter, Y., & Johansson, L. C. (2012). Kinematics and wing shape across flight speed in the bat, *Leptonycteris yerbabuenae*. *Biology Open*, *1*(12), 1226–1238. http://doi.org/10.1242/bio.20122964

Von der Emde, G. (1999). Active electrolocation of objects in weakly electric fish. *Journal of Experimental Biology*, *202*(10), 1205–1215.

Von der Emde, G., & Schnitzler, H.-U. (1990). Classification of insects by echolocating greater horseshoe bats. *Journal of Comparative Physiology A: Neuroethology, Sensory, Neural, and Behavioral Physiology*, *167*(3), 423–430. http://doi.org/10.1007/BF00192577

Wang, Z. J. (2000). Vortex shedding and frequency selection in flapping flight. *Journal of Fluid Mechanics*, *410*, 323–341. http://doi.org/10.1017/S0022112099008071

Warrick, D. R., Tobalske, B. W., & Powers, D. R. (2005). Aerodynamics of the hovering hummingbird. *Nature*, *435*(7045), 1094–1097. http://doi.org/10.1038/nature03647

Weis-Fogh, T., & Jensen, M. (1956). Biology and Physics of Locust Flight. I. Basic Principles in Insect Flight. A Critical Review. *Philosophical Transactions of the Royal Society of London. Series B, Biological Sciences*, *239*(667), 415–458.

Wilson, W., & Moss, C. F. (2004). Sensory-motor behavior of free-flying FM bats during target capture. In J. A. Thomas, C. F. Moss, & M. Vater (Eds.), *Echolocation in bats and dolphins* (pp. 22–27). Chicago University Press.

Wolf, M., Johansson, L. C., Von Busse, R., Winter, Y., & Hedenström, A. (2010). Kinematics of Flight and the Relationship to the Vortex Wake of a Pallas' Long Tongued Bat (*Glossophaga Soricina*). *Journal of Experimental Biology*, *213*(12), 2142–2153. http://doi.org/10.1242/jeb.029777